Water Resources Research

RESEARCH ARTICLE
10.1029/2020WR027992

Disentangling the Impact of Catchment Heterogeneity on Nitrate Export Dynamics From Event to Long-Term Time Scales

Carolin Winter[1], Stefanie R. Lutz[1], Andreas Musolff[1], Rohini Kumar[2], Michael Weber[2], and Jan H. Fleckenstein[1,3]

[1]Department for Hydrogeology, Helmholtz Centre for Environmental Research—UFZ, Leipzig, Germany, [2]Department for Computational Hydrosystems, Helmholtz Centre for Environmental Research—UFZ, Leipzig, Germany, [3]Bayreuth Center of Ecology and Environmental Research, University of Bayreuth, Bayreuth, Germany

Key Points:

- Analyzing the *CQ* relationship across time scales allows the disentanglement of the impact of catchment heterogeneity on nitrate export
- Mountainous upstream subcatchments can dominate nitrate export during high flows and disproportionally contribute to nitrate loads
- Agricultural downstream subcatchments can dominate nitrate export during low flow and pose a long-term threat to water quality

Supporting Information:

- Supporting Information S1

Correspondence to:
C. Winter,
carolin.winter@ufz.de

Citation:
Winter, C., Lutz, S. R., Musolff, A., Kumar, R., Weber, M., & Fleckenstein, J. H. (2021). Disentangling the impact of catchment heterogeneity on nitrate export dynamics from event to long-term time scales. *Water Resources Research*, *57*, e2020WR027992. https://doi.org/10.1029/2020WR027992

Received 21 MAY 2020
Accepted 3 DEC 2020

Abstract

Defining effective measures to reduce nitrate pollution in heterogeneous mesoscale catchments remains challenging when based on concentration measurements at the outlet only. One reason for this is our limited understanding of the subcatchment contributions to nitrate export and their importance at different time scales. While upstream subcatchments often disproportionally contribute to runoff generation and in turn to nutrient export, agricultural areas (which are typically found in downstream lowlands) are known to be a major source of nitrate pollution. To examine the interplay of different subcatchments, we analyzed seasonal long-term trends and event dynamics of nitrate concentrations, loads, and the concentration–discharge relationship in three nested catchments within the Selke catchment (456 km^2), Germany. The upstream subcatchments (40.4% of total catchment area, 34.5% of N input) had short transit times and dynamic concentration–discharge relationships with elevated nitrate concentrations during wet seasons and events. Consequently, the upstream subcatchments dominated nitrate export during high flow and disproportionally contributed to overall annual nitrate loads at the outlet (64.2%). The downstream subcatchment was characterized by higher N input, longer transit times, and relatively constant nitrate concentrations between seasons, dominating nitrate export during low-flow periods. Neglecting the disproportional role of upstream subcatchments for temporally elevated nitrate concentrations and net annual loads can lead to an overestimation of the role of agricultural lowlands. Nonetheless, constantly high concentrations from nitrate legacies pose a long-term threat to water quality in agricultural lowlands. This knowledge is crucial for an effective and site-specific water quality management.

Plain Language Summary

To efficiently remove nitrate pollution, we need to understand how it is transported, mobilized, and stored within large and heterogeneous catchments. Previous studies have shown that upstream catchments often have a disproportional impact on nutrient export, while agriculture (a major nitrate source) is often located in downstream lowlands. To understand which parts of a catchment contribute most to nitrate export and when, we analyzed long-term (1983–2016) and high-frequency (2010–2016) data in the Selke catchment (Germany) at three locations. The mountainous upstream part dominated nitrate transport during winter, spring, and rain events. It had a surprisingly high contribution to annual nitrate loads. The agricultural downstream part of the catchment dominated nitrate export during summer and autumn, with relatively constant concentrations between seasons. Here, nitrogen inputs needed more than a decade to travel through the subsurface of the catchment, which causes a time lag between measures to reduce nitrate pollution and their measurable effect. The resulting storage of nitrate in the groundwater threatens drinking water quality for decades to come. While the role of agricultural lowlands for nitrate export can be overestimated if neglecting the disproportional role of upstream subcatchments, their impact poses a long-term threat to water quality.

1. Introduction

High nitrate concentrations in ground water and surface water are a well-known but still widespread problem in most developed countries (Bouraoui & Grizzetti, 2011; Kohl et al., 1971; Rockström et al., 2009). These high concentrations pose a threat to our drinking water quality and the integrity of aquatic ecosystems

(Camargo & Alonso, 2006; Majumdar & Gupta, 2000). To most efficiently reduce nitrate pollution, a detailed understanding of the catchment-internal processes that drive nitrate mobilization, transport, storage, and transformation is needed. While much is known about these processes for rather uniform headwater catchments, our understanding of those in spatially more heterogeneous and complex mesoscale catchments (10^1–10^4 km^2, Breuer et al., 2008) is yet an open challenge but vital for identifying management options. On the one hand, upstream subcatchments often have a disproportional contribution to runoff generation due to their higher drainage density and in turn they often disproportionally contribute to nutrient mobilization and transport (e.g., Alexander et al., 2007; Dodds & Oakes, 2008; Goodridge & Melack, 2012). On the other hand, agricultural areas are known to be a major source of nitrate pollution (e.g., Padilla et al., 2018; Strebel et al., 1989). A typical setting for mesoscale catchments located in the transition zone between uplands and lowlands is, however, an elevated upstream area with no or only a small percentage of agricultural land use and a downstream lowland area where agricultural land use dominates (e.g., Krause et al., 2006; Montzka et al., 2008). Hence, the different upstream and downstream subcatchments can have quite different nitrate export dynamics. Both subcatchments are relevant for nitrate export from the entire catchment and may operate at very different times and time scales. Their specific contributions, however, remain widely unknown when measuring only the integrated signal of nitrate export at the catchment outlet, making it difficult to localize important source zones of nitrate and to identify important driving forces for their mobilization. Nested catchment studies are a promising approach to shedding light on the contribution of subcatchments to nitrate export (e.g., Dupas et al., 2017; Ehrhardt et al., 2019). They enable us to analyze changes in nitrate transport along the river, to connect these changes to the specific characteristics of upstream and downstream subcatchments and to interpret the integrated observations of concentration, discharge (Q), and loads at the catchment outlet.

1.1. Time Scales of Nitrate Export

The dynamics of water quality can be assessed on various time scales, which all have their specific relevance for understanding nitrate export dynamics at catchment scale. Long-term data are indispensable for assessing trends in water quality over time and for assessing transit times (TTs) and legacy stores, both of which can delay or buffer the catchment response to solute input at the catchment outlet (Dupas et al., 2016; Hirsch et al., 2010; Van Meter et al., 2017). Here, we refer to TTs as the time lag between the introduction of a solute into the catchment and its riverine export, leading to a temporal storage of N in the catchment. Legacy stores refer to the mass of solute that has been retained and accumulated in the catchment. In the case of N, legacy stores are separated into organic N retained in the soil (biogeochemical legacy) and inorganic N that is moving in the groundwater (hydrological legacy) with TTs that strongly depend on catchment-specific characteristics such as recharge and the storage capacity (Haitjema, 1995). A precise understanding of the contribution of TTs and legacy stores to nitrate export dynamics and the long-term persistence of nitrate is still missing (Van Meter et al., 2016). However, this knowledge is crucial for understanding the response of riverine nitrate concentrations to land use changes and the time scale between measures to reduce nitrate reduction and their measurable success. Moreover, understanding the controls on the long-term persistence of pollutants—such as nitrate—within catchments was just recently framed to be one of the major unsolved problems in hydrology (Blöschl et al., 2019).

Long-term data are most often available at a low frequency (weekly to monthly), as methods to continuously measure high-frequency nitrate concentrations have only recently been developed (Burns et al., 2019). While these long-term, low-frequency data are appropriate for the identification of long-term trends, TTs, and legacy stores (e.g., Ehrhardt et al., 2019; Hirsch et al., 2010), the analysis of event dynamics can only be conducted with high-frequency data (Burns et al., 2019). The time scale of single events, however, is especially important for the analysis of nitrate dynamics, because most of the annual nitrate load to the stream is transported during events (Bernal et al., 2002; Inamdar et al., 2006). Event dynamics of nitrate concentrations (C) and Q can shed light on mobilization and transport processes that are masked when only long-term trends are looked at (Duncan et al., 2017; Rose et al., 2018). For example, Dupas et al. (2016) found chemostasis (i.e., the variability of nitrate concentrations is low compared to that of Q and there is no significant directional relationship between C and Q) in long-term trends in a mesoscale catchment, while dynamics at the scale of discharge events conversely showed a decrease of nitrate concentrations with

increasing Q. They argued that these event-scale patterns are one of the main drivers for the uncertainty in annual load estimations. Moreover, both long-term trends and event dynamics often show a strong seasonality (e.g., Dupas et al., 2017) which should be analyzed in parallel in order to be able to accurately assess nitrate export patterns across time scales. Consequently, a combination of analyses of all (long-term trends, event dynamics, and their seasonality) is needed to address the knowledge gap in driving forces of nitrate export dynamics.

1.2. Concentration–Discharge Relationship

The concentration–discharge relationship (*CQ* relationship) is a simple data-driven concept that is commonly used to investigate export dynamics of nitrate and other solutes on various spatial and temporal scales (e.g., Godsey et al., 2009; Musolff et al., 2015; Rose et al., 2018). In general, the *CQ* relationship allows differentiation between three different export regimes: (i) chemodynamic with accretion pattern, (ii) chemodynamic with dilution pattern, and (iii) chemostasis (Godsey et al., 2009; Musolff et al., 2017). Export regimes (i) and (ii) are both summarized under the term "chemodynamic," which means that a solute's concentration variability is comparable to or higher than the variability of Q, with concentrations either increasing (accretion) or decreasing (dilution) with increasing Q. Accretion patterns are generally explained by additional source zones becoming connected during higher flow conditions, while dilution patterns are observed when higher Q causes a dilution of instream solute concentrations without further source zone activation (Basu et al., 2010). Chemodynamic nitrate export has often been found in relatively natural systems with no or only a small percentage of agricultural land use or urban areas, i.e., where nitrate sources are not ubiquitously available (Basu et al., 2010; Goodridge & Melack, 2012). On the contrary, chemostasis indicates constant nutrient concentrations instream that are not significantly correlated to Q and have a considerably lower variability (Basu et al., 2010; Bieroza et al., 2018). This pattern often emerges in catchments with a spatially uniform distribution of abundant solute sources, such as nitrate in agricultural areas, leading to a relatively constant release of solutes to the stream network (Basu et al., 2010; Bieroza et al., 2018). To assess the directional relationship between C and Q, Godsey et al. (2009) proposed a power law relationship between C and Q, with the corresponding slope between $\ln(C)$ and $\ln(Q)$ termed the *CQ* slope. Subsequently, Thompson et al. (2011) established the CV_C/CV_Q metric to express the variability in C relative to the variability in Q (with CV being the coefficient of variation). Jawitz and Mitchell (2011) and Musolff et al. (2015) combined the two approaches to a single conceptual framework as *CQ* slope and CV_C/CV_Q are mathematically linked.

So far, top-down assessments of catchment export dynamics have mainly been focused on observations at the catchment outlet, largely neglecting catchment-internal variabilities. Here, we see the need for research on how the role of internal organization of catchments (i.e., nested subcatchments) shapes the outlet observation seasonally and under varying flow conditions in terms of nitrate inputs, reactive transport in the subsurface, and the stream network. To address this research gap, we conduct a nested catchment study in the mesoscale Selke catchment, which is an intensively monitored research site (Jiang et al., 2014; Wollschläger et al., 2017) that provides the unique opportunity to study long-term trends as well as event-scale nitrate concentrations and loads. We analyzed (i) seasonal long-term trends and (ii) event dynamics of nitrate concentrations, loads, and the *CQ* relationship for each nested subcatchment. Furthermore, we (iii) calculated subcatchment-specific transit time distributions (TTDs) from N inputs and riverine nitrate outputs to address the potential extent and effect of legacy stores and their impact on nitrate export dynamics and long-term trends. Using this comprehensive approach, our aim was to obtain a better understanding of how nested subcatchments (i) contribute to the integrated signal of nitrate concentrations, loads, and *CQ* relationships observed at the catchment outlet at different times scales (long term, seasonal, and event scale), and how they (ii) affect the response of nitrate concentrations, loads, and *CQ* relationships to changes in N input.

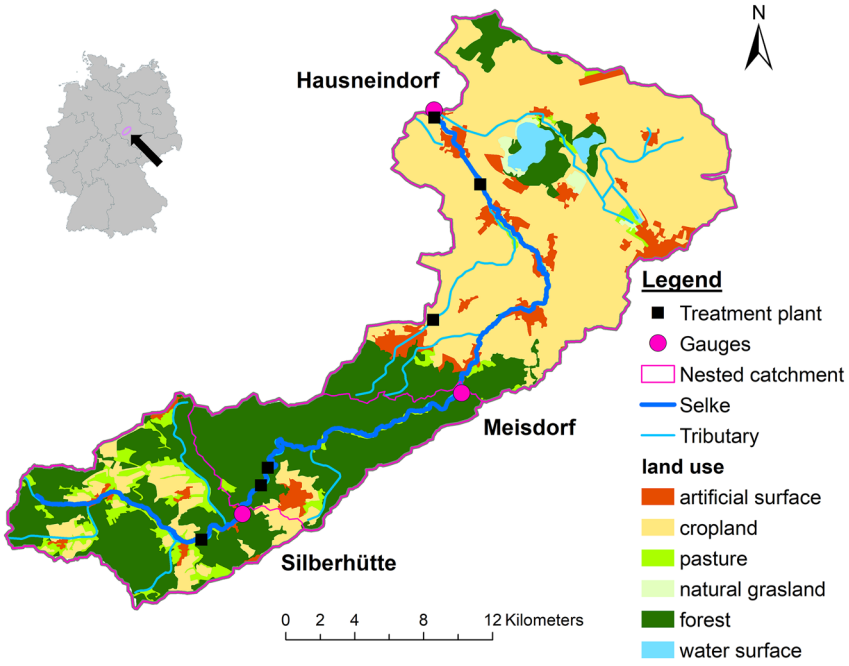

Figure 1. Land use map of the Selke catchment with gauging stations (pink dots) and wastewater treatment plants (black squares).

2. Materials and Methods

2.1. Catchment Description

The Selke catchment is located in the Harz Mountains and the Harz foreland of Saxony-Anhalt, Germany (Figure 1). It is a subcatchment of the Bode catchment, which is an intensively monitored catchment within the network of TERrestrial ENvironmental Observatories (TERENO, Wollschläger et al., 2017). We considered three nested subcatchments in the Selke catchment (Figure 1 and Table 1), delineated by the following gauging stations: (i) Silberhütte, (ii) Meisdorf, and (iii) Hausneindorf. Characteristics of the subcatchments are summarized in Table 1.

Silberhütte and Meisdorf are located in the Harz Mountains and drain the upper part of the catchment. In the following, these two nested subcatchments are summarized as the *upper Selke*. The upper Selke is dominated by forests, followed by agriculture, which is mainly located upstream of Silberhütte (Table 1). Soils are dominated by Cambisols overlaying low permeable schist and claystone, resulting in relatively shallow groundwater systems (Jiang et al., 2014). Due to the higher elevation (Table 1), a considerable amount of snowmelt contributes to stream discharge during late winter and spring (X. Yang et al., 2018). There are three wastewater treatment plants (WWTPs) located in the upper Selke, of which one is located at the upper part draining to the gauge in Silberhütte.

The transition from the upper to the lower part of the catchment marks a distinct change in landscape characteristics. The downstream part of the catchment is termed *lower Selke* from here on. It is a fertile plain with productive soils in the foreland of the Harz Mountains dominated by agriculture (Table 1) mainly in the form of arable crops. Soils are dominated by Chernozems above quaternary sediments and mesozoic sedimentary rocks (sandstone and limestone) that allow for considerably deeper groundwater systems than those found in the upper Selke (Jiang et al., 2014).

Another three WWTPs are located in the lower Selke, of which one is at a tributary to the Selke (Figure 1). Furthermore, there was an opencast mine (closed in 1991) located in the northeastern part of the lower Selke. Selke water has been abstracted from 1998 on to fill the open pit with an average annual abstraction rate

Table 1
Characteristics of the Three Nested Subcatchments Within the Selke Catchment

Catchment characteristic		Unit	Upper Selke		Lower Selke		Data source
					Hausneindorf		
			Silberhütte	Meisdorf	Nested[a]	Separate[a]	
Area		(km^2)	105	184	456	272	LHW[b]
MAP[c]		($mm\ year^{-1}$)	739.1	694.3	588.9	519.0	DWD[d], Zink et al. (2017)
Elevation range		(m.a.s.l.)	335–597	196–597	68–597	68–396	EEA (2013)[e]
Mean slope		(%)	6.9	8.4	4.9	2.7	EEA (2013)
Specific discharge		($mm\ day^{-1}$)	0.90	0.65	0.32		LHW
Land use	Agriculture	(%)	30.5	20.9	47.8	65.0	EEA (2012)
	Forest		65.0	75.3	39.8	17.1	
	Urban		3.3	3.1	5.9	7.7	
	Others		1.2	0.7	6.5	10.2	

Note. [a]Nested catchment characteristics for Hausneindorf (left column) integrate the upper Selke while the separate characteristics exclude the upper Selke (right column). Analysis and results in this study are based on the nested version. [b]State Office of Flood Protection and Water Management of Saxony-Anhalt. [c]Mean annual precipitation. [d]German Weather Service. [e]Digital elevation model of the European Environment Agency downscaled to a resolution of 100 m.

of 3.1 million m^3. In 2009, a landslide occurred on the banks of the pit-lake, so that water from the filling pit has been pumped (annual rate of 10.4 million m^3) into the Selke in order to stabilize the banks since 2010.

Note that due to the nested catchment structure, all measurements from the lower Selke are an integrated signal from the upper and the lower Selke.

2.2. Data Basis

Daily Q data are publicly available for all gauges from 1983 to 2016 and high-frequency Q data (15 min) are available since 2010. All data are provided by the State Office of Flood Protection and Water Management of Saxony-Anhalt (LHW; Figure S1). Long-term data of nitrate concentrations for all three gauges were provided by the LHW from 1983 to 2009 and by the Helmholtz Centre for Environmental Research (UFZ) from 2010 to 2016, collected as grab samples at biweekly to bimonthly intervals and published previously by X. Yang et al. (2018). Continuous high-frequency data of nitrate were measured in more recent years at 15 min intervals using TriOS ProPS-UV sensors (described in more detail by Rode et al., 2016). Sensor performance was reported to be high, with an R^2 of 0.93 for the regression of grab samples and sensor-derived concentrations ($y = 1.001x$, $n = 122$) and a bias of 0.01 mg NO_3^-N (Rode et al., 2016). The data were collected by the UFZ as part of the TERENO monitoring program from 2013 to 2016 for Silberhütte, October 2010 to 2016 for Meisdorf, and July 2010 to 2016 for Hausneindorf. Slight variations in the timing of measurements between Q and nitrate concentrations were corrected by aggregation to equal 15 min intervals.

2.3. Long-Term Trends of Concentrations and Concentration–Discharge Relationships

All analyses were carried out within the R software environment (R Core Team, 2019). Long-term trends in nitrate concentrations and loads were calculated using "Weighted Regression on Time, Discharge and Season" (WRTDS, Hirsch et al., 2010), implemented in the R package "Exploration and Graphics for RivEr Trends" (EGRET). WRTDS requires time, Q, and season as explanatory variables to simulate daily concentrations from sporadic measurements over long time series (Hirsch et al., 2010):

$$ln(C_i) = \beta_{0,i} + \beta_{1,i}t_i + \beta_{2,i}ln(Q_i) + \beta_{3,i}sin(2\pi t_i) + \beta_{4,i}cos(2\pi t_i) + \varepsilon_i \quad (1)$$

where subscript i indicates the specific day, C is the concentration in mg L^{-1}, t is the time in decimal years, Q is the discharge in $m^3\ s^{-1}$, β_1–β_4 are fitted coefficients with β_2 representing the CQ slope, and ε is an error term.

The regression in WRTDS is weighted via the tricube weight function (Tuckey, 1977), which gives an increasing weighting to observations close to the estimation point in terms of time, Q, and season (Hirsch et al., 2010). Flow normalization is applied for an estimation of concentration that is unbiased by daily Q variation. Here, concentrations are flow normalized (FN) in such a way that measured Q on a given date is assumed to have the same probability as all observed Q values of that date in all other years in the record. Thus, for every single date in the time series, Equation 1 is applied once with every Q record that was measured on the same date in all years and these values are finally averaged to one single FN concentration estimate for the specific day.

In order to analyze long-term trends of the CQ relationship, we used a modification of the original EGRET codes to extract the daily parameter β_2 from Equation 1 (which was developed by Zhang et al., 2016). The parameter β_2 represents the relationship between ln(C) and ln(Q) (CQ slope), which enables a differentiation between export regimes: (i) chemodynamic with an accretion pattern ($\beta_2 > 0.1$), (ii) chemodynamic with a dilution pattern ($\beta_2 < -0.1$), and (iii) chemostatic ($-0.1 < \beta_2 < 0.1$). We chose the threshold for chemostatic at −0.1 and 0.1 as according to Zhang et al. (2016) and Bieroza et al. (2018), although we are aware that this somewhat arbitrary threshold only indicates chemostatic patterns if $CV_C/CV_Q << 1$ (Musolff et al., 2015). The CQ slope and the CV_C/CV_Q were found to be positively correlated for nitrate (Musolff et al., 2015), as most of the variability in C is explained by variability in Q. In this case, the additional information gained by the CV_C/CV_Q metric is small. The methods and results of this study are therefore restricted to the CQ slope.

Using daily streamflow data and low-frequency nitrate concentrations, we calculated seasonally averaged and FN nitrate concentrations, loads, and FN CQ slopes for all gauges from 1983 to 2016 in order to detect long-term trends and seasonal differences. Spring was defined as lasting from March to May, summer from June to August, autumn from September to November, and winter from December to February. To quantify the uncertainty, all results were bootstrapped 200 times using the R package EGRETci (Hirsch et al., 2015) for FN nitrate concentrations and loads and a modification of the code from Zhang et al. (2016) for bootstrapping β_2. As recommended by Hirsch et al. (2015), we used a block length of 200 (randomly selected with replacement) and show the 90% confidence interval in all consequent figures (5%–95% quantiles).

2.4. Nitrogen Input

N input into the Selke catchment was calculated following the procedure described by Ehrhardt et al. (2019). Here, N input refers to N surplus as the sum of three different input classes: (i) agricultural N surplus, (ii) atmospheric N deposition, and (iii) N input from WWTPs, where (i) and (ii) are diffuse sources and (iii) is a point source. To stay consistent with the nested catchment structure, N input data of Meisdorf represent N input for the entire upper Selke and N input from the lower Selke represents the entire Selke catchment, including the upper part.

We used agricultural N surplus data derived for the 403 counties in Germany, representing the annual surplus of N on agricultural areas that results from the difference between N sources (i.e., fertilizer and manure application, atmospheric deposition, and biological N fixation by legumes) and N sinks in the form of N in harvested crops (Bach & Frede, 1998; Behrendt et al., 2000; Häußermann et al., 2019). Our study area covers three counties. The share of agricultural area for each county was taken from the CORINE Land Cover (CLC, EEA, 2012) for the years 1990, 2000, 2006, and 2012 and further corrected as according to Bach et al. (2006, personal communication), introducing a scaling factor for each county to adjust for the mismatch between the CLC-derived agricultural share and that from statistical data sources (Bach et al., 2006).

Atmospheric N deposition represents the annual input from N emissions due to burning in private households, industry, and traffic between 1980 and 2015, the data were provided by the Meteorological Synthesizing Centre – West of the European Monitoring and Evaluation Programme (e.g., Bartnicky & Ben-

edictow, 2017; Bartnicky & Fagerli, 2004). From 1950 to 1980, the county-based input is assumed to be constant (25.03 kg ha^{-1} $year^{-1}$ in Silberhütte, 28.75 kg ha^{-1} $year^{-1}$ in Meisdorf and 16.15 kg ha^{-1} $year^{-1}$ in Hausneindorf) due to a lack of further data for that time. We considered N deposition data only for nonagricultural land cover classes (e.g., forest, water bodies, wetlands, and grassland) because the agricultural N surplus data already account for atmospheric deposition and biological fixation (see above). We added biological N fixation to nonagricultural land cover classes according to Cleveland et al. (1999) and Van Meter et al. (2017). Cities were neglected (except urban grassland such as parks) under the assumption that nitrogen from sealed surfaces is directly discharged into the WWTPs. We acknowledge that sealed-surfaces runoff which enters directly into the stream can have a considerable impact (Decina et al., 2018; Hope et al., 2004). However, due to the small percentage of urban areas in the Selke catchment (5.9%, Table 1), we believe that this simplification is acceptable.

Data on the annual mean nitrate and ammonium concentrations from WWTP outflow between 2010 and 2015 were provided by the Ministry of Environment, Agriculture and Energy Saxony-Anhalt. We calculated nitrate input from WWTPs with the provided nitrate concentrations and an additional maximum estimate for the contribution of WWTPs to nitrate export during high-flow seasons (HFSs) and low-flow seasons (LFSs) under the assumption of a complete nitrification of wastewater-borne ammonium. Nitrate concentration values from 2010 were assigned to all years previous to 2010. As their contribution to N input in the Selke catchment is relatively small, compared to agricultural N input, we believe that these data and their extrapolation robustly represent the recent state of point source N loads but do not allow for describing the long-term evolution of N loads due to improvements in wastewater treatment and newly constructed WWTPs.

Finally, a harmonized and consistent data set for each of the three different input types was created on county level (average area of 887 km^2) for the period of 1950–2015 and combined to one single N input data set that was clipped for all three nested subcatchments. To this end, we used the weighted average, taking into account the areal fractions of involved counties and the respective (sub)catchment boundaries. To compare N input with nitrate export, we assume that entire N input is eventually mineralized and that nitrate concentration patterns (with nitrate as the most abundant species of inorganic N, Meybeck, 1982) reflect the main processes of riverine N export and subcatchment-specific differences in N export dynamics. To account for this simplification, we discuss other important processes that play a role in reactive N transport, such as instream assimilation or denitrification in riparian zones.

2.5. Transit Time Distributions

Apparent TTDs for nitrate were calculated by applying a methodology described by Musolff et al. (2017) and Ehrhardt et al. (2019). We assumed a log-normal form for the TTDs because this allows us to account for the long tails in the TTD needed to adequately reflect legacy effects. First, we scaled N input and mean annual FN nitrate concentrations from the long-term low-frequency data in order to compare the temporal dynamics of input and output independently from their absolute value. Then, we calibrated the parameters μ and σ of the log-normal distribution (mean and standard deviation of the natural logarithm of the target variable, defining the tailing and mode) by minimizing the sum of squared errors between simulated and measured scaled FN nitrate concentrations. We used these TTDs to compare the response of the nested catchments to changes in N input and to improve our estimate of N legacies in the period from 1983 to 2015. More specifically, we calculated the total conservative N export for each subcatchment by convolving the annual N input for each year with the calibrated TTDs, extracting the fractions that would be exported by 2015 and summing up these annual estimates to derive the cumulative N export until 2015. We then compared this estimate of conservative N export to the measured nitrate export over the same period to get an estimate of the *missing N*. We assume that *missing N* was either removed via denitrification or that it is still in the catchment as hydrological legacy (delayed by long TTs of subsurface water i.e., hydrological TTs) or as biogeochemical legacy (stored as organic N in the catchment soils). Determining which form of legacy the *missing N* can be contributed to is challenging (Van Meter & Basu, 2015; Van Meter et al., 2016) and beyond the scope of this study. Nevertheless, long-term trends in *CQ* relationships together with pronounced changes in N input can give first indications on their contribution (Ehrhardt et al., 2019). In respect to hydrological legacies, a decline in N input can cause a temporal increase in the concentration heterogeneity

belowground (e.g., between younger and older water fractions), which can go along with a shift in *CQ* relationships from chemostasis toward more chemodynamic patterns. In contrast, *CQ* relationships under the dominance of biogeochemical legacies are likely to be more buffered and less affected by changes in N input (Ehrhardt et al., 2019). Hence, we used long-term trends in the *CQ* slope to discuss indications toward either hydrological or biogeochemical legacies. Additionally, we compared the difference between TTD-derived and measured N export to literature data on potential denitrification.

2.6. Event Dynamics

We used the high-frequency data from 2010 to 2016 to analyze storm events at all three gauges. To identify events, we converted Q from $m^3\ s^{-1}$ to mm, smoothed it with a running average and separated it into a base flow and fast flow component following the methodology described by Gustard (1983) and WMO (2008). This methodology linearly interpolates between turning points in Q that are defined as local minima (within a nonoverlapping 5-day window) which are at least 1.11 times smaller than their neighboring minima. Despite its simplicity, this base flow separation method was chosen because it permits an unambiguous identification of event starting points (Tarasova et al., 2018). We defined the start of an event as the point in time when fast flow increases to at least 2.5% of base flow and Q has increased by a minimum of 5% over the previous 5 h. Events were defined to end when fast flow decreases to less than 2.5% of base flow. The final selection of the event was based on the criteria that (i) the event included a minimum of 20 data points, (ii) peak Q reached at least the 5% percentile of all Q measurements, (iii) fast flow contribution at the peak of the event was at least 30% of total flow, and (iv) Q decreased at least to one third of its former increase. Events with data gaps larger than 5 h were discarded from the analysis. These criteria and thresholds were chosen as they allowed for a good balance between the separation of clearly evident events (from scatter in Q) and the detection of a sufficient number of small-scale events that occurred during LFSs to obtain a fairly equal number of events during all four seasons.

Next, we fitted Equation 2 to each selected event (Eder et al., 2010; Krueger et al., 2009; Minaudo et al., 2017) to analyze the event-specific *CQ* slope and the hysteresis direction and extent:

$$C = a * Q^b + c * \frac{dQ}{dt} \tag{2}$$

where a, b, and c are parameters that were fitted for each event individually. Parameter a gives the event-specific intercept and b the *CQ* slope, which is comparable to the parameter β_2 from the long-term analysis (Equation 1). Consequently, parameter b was used to differentiate between chemodynamic accretion ($b > 0.1$), chemodynamic dilution ($b < -0.1$), and chemostatic ($-0.1 < b < 0.1$) nitrate transport during storm events. Parameter c was used to identify the extent and direction of event-specific hysteresis with $c > 0.1$ indicating clockwise hysteresis, $c < -0.1$ indicating counterclockwise hysteresis and $-0.1 < c < 0.1$ indicating no or complex hysteresis. Note that dQ/dt was scaled for the individual event to allow a better comparison of c between the events. The season of an event was defined as the season in which the event starts. To assure the quality of results, parameters b and c were only used for further analysis if the coefficient of determination (R^2) for the event-specific fit of Equation 2 was larger than 0.5.

3. Results

3.1. Nitrogen Budget

Since the start of the N input time series in 1950, N input strongly increased until 1976 and fluctuated between 1976 and 1989 around an average N input of 57.3 kg ha^{-1} $year^{-1}$ in the upper Selke and 79.4 kg ha^{-1} $year^{-1}$ in the lower Selke. Maximum N input was reached in 1988. In 1990, after the reunification of Germany and the associated breakdown of the intensive agriculture in East Germany (Gross, 1996), N input decreased markedly within 1 year and then stabilized again at a lower level (around 33.9 ± 3.3 kg ha^{-1} $year^{-1}$ in the upper Selke and 37.7 ± 5.2 kg ha^{-1} $year^{-1}$ in the lower Selke) from 1995 onwards (Figure 2 and Table 2).

Annual N input per hectare (ha) was generally lower for the upper Selke (representing the catchment area draining to the gauge at Meisdorf) than for the lower Selke (representing the entire catchment area draining

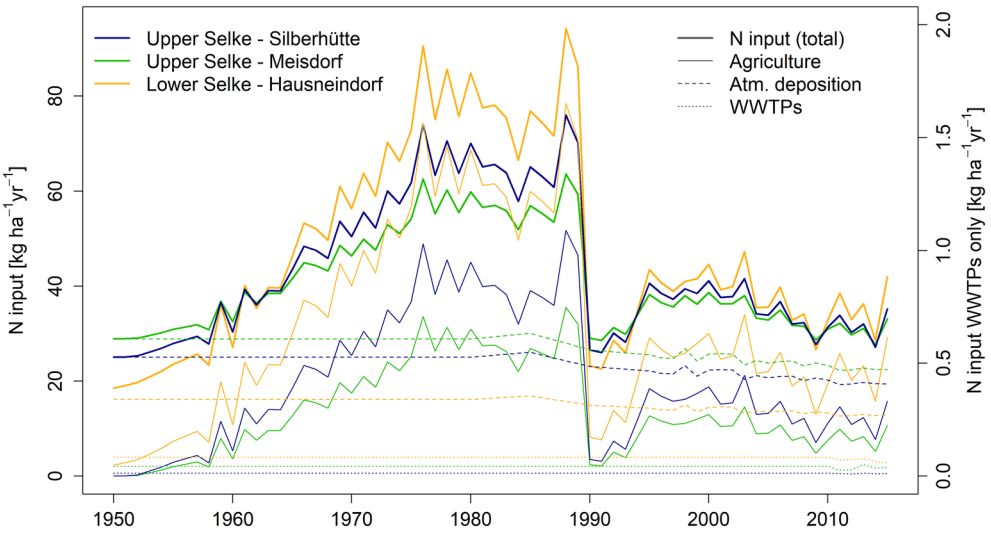

Figure 2. Total N input per hectare and year for all three nested subcatchments of the Selke catchment and N input divided into its components: (i) from agricultural areas, (ii) atmospheric deposition and biological fixation on nonagricultural areas, and (iii) outflow from wastewater treatment plants (WWTPs, second *y* axis).

to the gauge at Hausneindorf; Figure 2 and Table 2). The only exceptions were found during years when the total N input was especially low (e.g., 1990/1991). In these years, the scenario was reversed, with the highest N input in the upper Selke and the lowest N input in the lower Selke, due to a relatively high atmospheric N deposition over the Harz Mountains and biological N fixation in the forests (Figure 2 and Table 2). Between 1983 and 2015, approximately one third (34.5%) of N input stemmed from the upper Selke and most of this from the upstream area draining to the gauge at Silberhütte (Table 2). N surplus from agriculture in this period was around 33% and 68% of the total N input for the upper and lower Selke, respectively. The remaining N input mainly stemmed from natural areas (mainly forests and grasslands), while the contribution of WWTPs was small. When assuming constant N input from WWTPs over the year, they contributed an average of 0.8%–1.6% to exported annual nitrate loads in the upper Selke and 2.4%–3.6% in the lower Selke (assuming no or a complete nitrification of wastewater-born ammonium). During LFSs, the contribution of WWTPs to nitrate export was an average of 3.4%–7.4% and 6.2%–9.5% for the upper and lower Selke, respectively.

3.2. Seasonal and Long-Term Patterns in Nitrate Concentrations

Referring to the regular monitoring results between 1983 and 2016, the upper Selke showed a pronounced seasonality, with lower nitrate concentrations during LFSs (summer and autumn) and higher concentrations during HFSs (winter and spring), while nitrate concentrations in the lower Selke were more stable between seasons. In general, the fitted nitrate concentrations increased from the upper to the lower Selke (Figure 3), but due to the differences in seasonality, this increase was especially pronounced during LFSs. Here, FN nitrate concentrations (NO_3-N) ranged between 0.5 and 1.8 mg L^{-1} in the upper Selke and between 2.0 and 3.7 mg L^{-1} in the lower Selke. During HFSs, the difference between upper and lower Selke nitrate concentrations was relatively small. Here, FN nitrate concentrations ranged between 1.6 and 3.4 mg L^{-1} in the upper Selke and between 2.4 and 3.7 mg L^{-1} in the lower Selke. Using WRTDS to fit daily nitrate concentrations resulted in a small bias of 1.7%, 0.5%, and −0.5% for Silberhütte, Meisdorf and Hausneindorf, respectively, with respect to the measured long-term data.

Besides general differences in nitrate concentrations and their different seasonalities, long-term trends also showed varying behavior between upper and lower Selke, again most pronounced during LFSs. Here, a marginal decrease beginning in 1990 occurred in the upper Selke, while FN nitrate concentrations increased substantially in the lower Selke, with a maximum value of 3.7 and 3.5 mg L^{-1} in summer and autumn 1997, respectively. A secondary peak occurred during 2010, with 3.1 mg L^{-1} in both seasons (Figures 3c and 3d).

Table 2
Balance Between Nitrogen (N) Input and Its Riverine Export as Nitrate Loads and Transit Time Distributions (TTDs)

			Upper Selke		Lower Selke
		Unit	Silberhütte	Meisdorf	Hausneindorf
N input vs. export (1983–2015)	Cumulative N input	(t)	14,078.7	23,195.4	67,146.9
	$N\ export_{conv}$ (conservative)	(kg ha^{-1} $year^{-1}$)	44.3	41.2	50.3
	Cumulative $N\ export_{conv}$ (conservative)	(t)	15,352.9	25,045.3	75,753.0
	Cumulative N export, (measured)	(t)	3,052.1	3,912.0	6,094.3
	Missing N (conservative – measured)	(kg ha^{-1} $year^{-1}$)	35.5	34.8	46.3
		(t)	12,300.7	21,133.3	69,658.6
		(%)	80.1	84.4	92.0
TTDs	μ	(year)	2.12	1.59	2.91
	σ	(year)	1.15	1.10	0.73
	R^2	(–)	0.57	0.92	0.40
	Mode (year of peak travel time)	(year)	3	3	12

Note. Conservative N export is the N input convolved with TTDs as indicated by subscript conv. Missing N refers to the difference between conservative N export and measured N export in form of riverine nitrate loads. TTDs follow a log-normal distribution with fitted parameters μ and σ and the R^2 as the coefficient of determination.

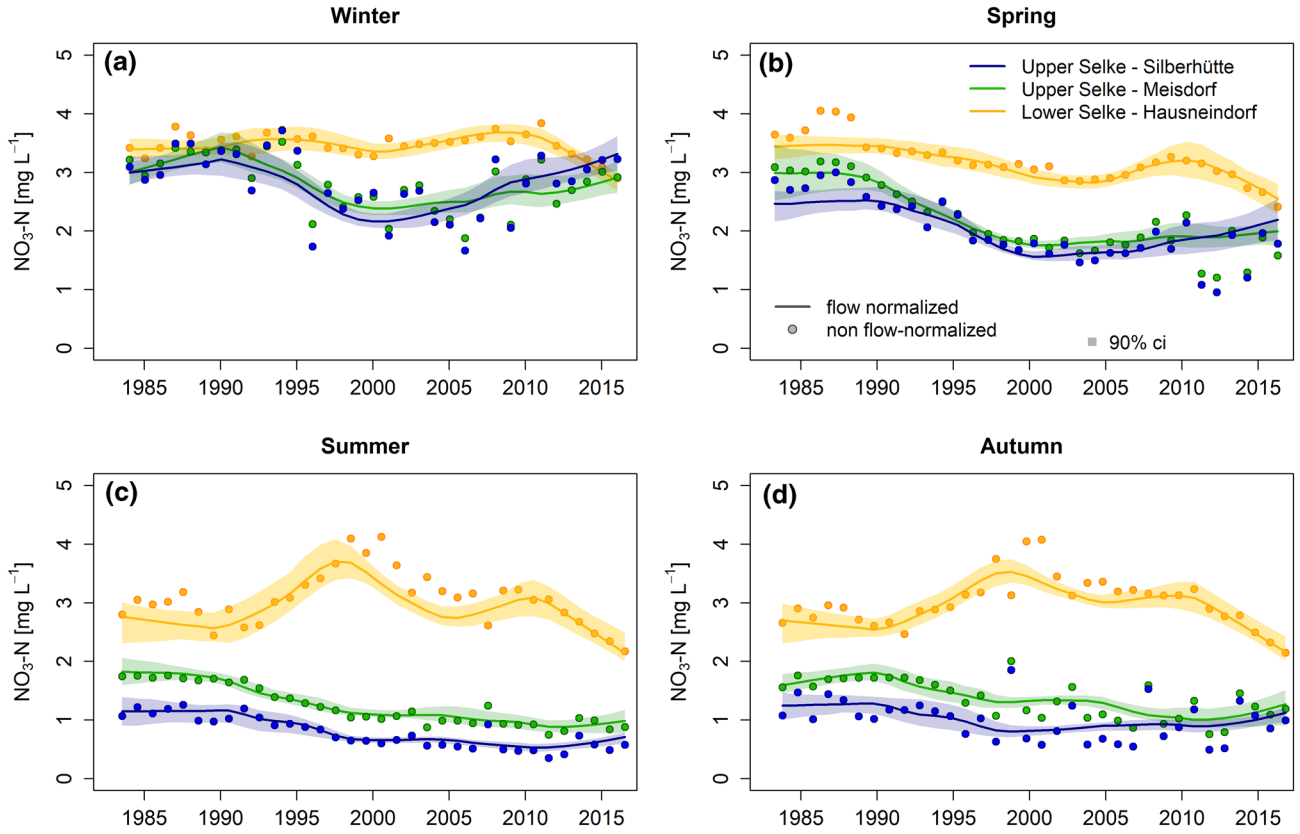

Figure 3. Long-term trends of annual flow normalized (FN, lines) and annual non-FN (dots) nitrate concentrations from three nested subcatchments of the Selke catchment, separated by season (a–d). Uncertainty bands in the subcatchment-specific color indicate the 90% confidence intervals from bootstrapping FN values.

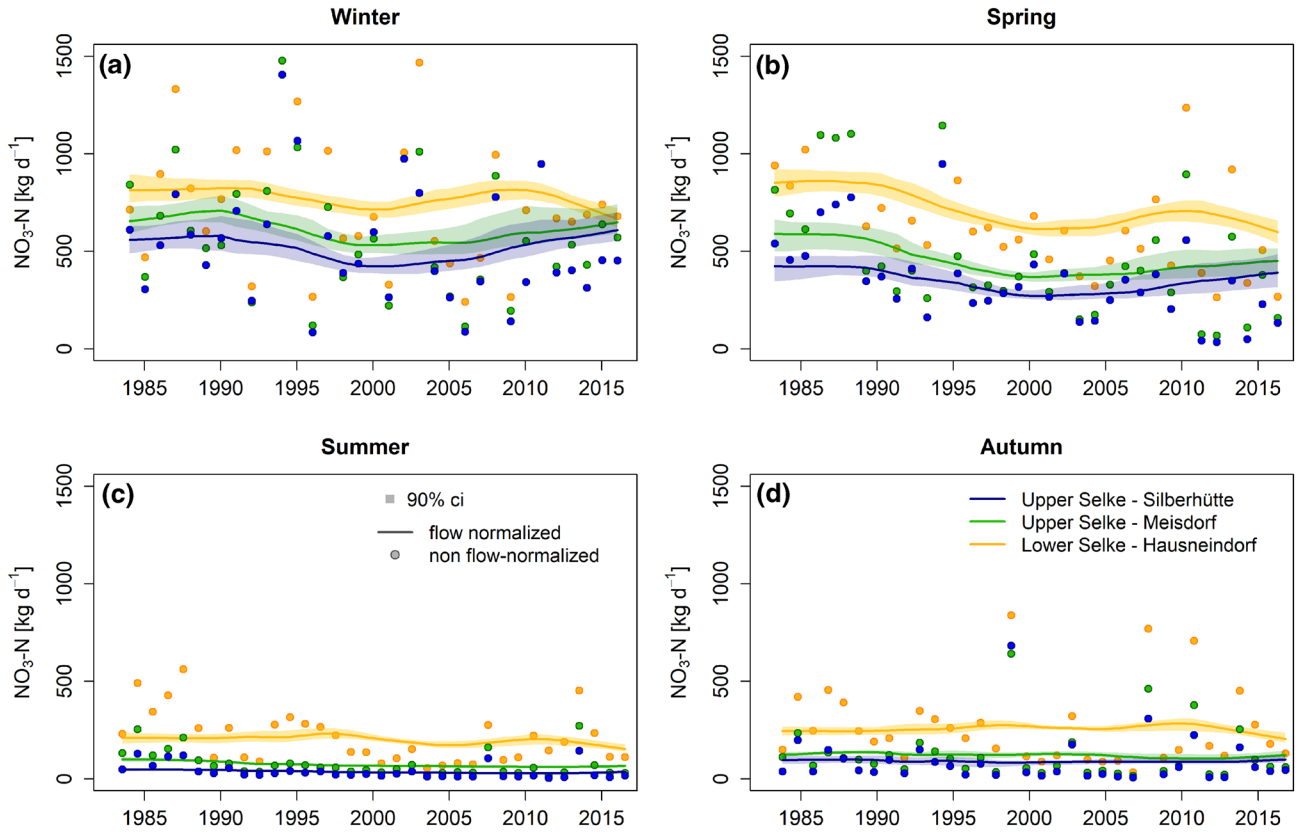

Figure 4. Long-term trends in annual flow normalized (FN, lines) and annual non-FN (dots) nitrate loads from three nested subcatchments of the Selke catchment, separated by season (a–d). Uncertainty bands in the subcatchment-specific color indicate the 90% confidence intervals from bootstrapping FN values.

In the most recent years (2011–2016), nitrate concentrations in the lower Selke during LFSs decreased to an average value of 2.6 mg L^{-1}. During HFSs, nitrate concentrations in the upper Selke decreased more strongly after 1990 but increased again staring in 2000. In the lower Selke, however, only slight temporal changes occurred during HFSs and the decrease in most recent years (observable during LFSs) occurred to a lesser extent also during HFSs (Figures 3a and 3b).

3.3. Seasonal and Long-Term Behavior of Nitrate Loads

Nitrate loads generally showed similar long-term trends than nitrate concentrations did (Figure 4). The main difference was in the pronunciation of seasonality, with much higher loads during HFSs compared to LFSs (Figure 4). This seasonality was even more pronounced in the upper Selke than in the lower Selke, and the relative contribution from subcatchments to nitrate loads varied seasonally in consequence. Overall, highest loads occurred during winter, with an average of 515.5 kg day^{-1} in Silberhütte, 607.8 kg day^{-1} in Meisdorf, and 774.8 kg day^{-1} in Hausneindorf (average from non-FN values). When neglecting in-stream losses of nitrate, this implies that the upper Selke transported 78.4% of the total catchment's nitrate loads which are exported from the lower Selke during winter (1983–2016). Lowest loads occurred during summer with 39.5 kg day^{-1}, 77.4 kg day^{-1}, and 207.6 kg day^{-1} for Silberhütte, Meisdorf, and Hausneindorf, respectively. Contrary to the situation in winter, the upper Selke had a much smaller contribution to the catchments loads of only 37.3% during summer. On an annual scale, the upper Selke contributed approximately 64.2% to the total catchment's nitrate loads. When taking the subcatchment area into account, the average of annual loads was highest in Silberhütte with 8.6 kg ha^{-1} $year^{-1}$, followed by Meisdorf with 6.3 kg ha^{-1} $year^{-1}$ and smallest in Hausneindorf with 3.9 kg ha^{-1} $year^{-1}$.

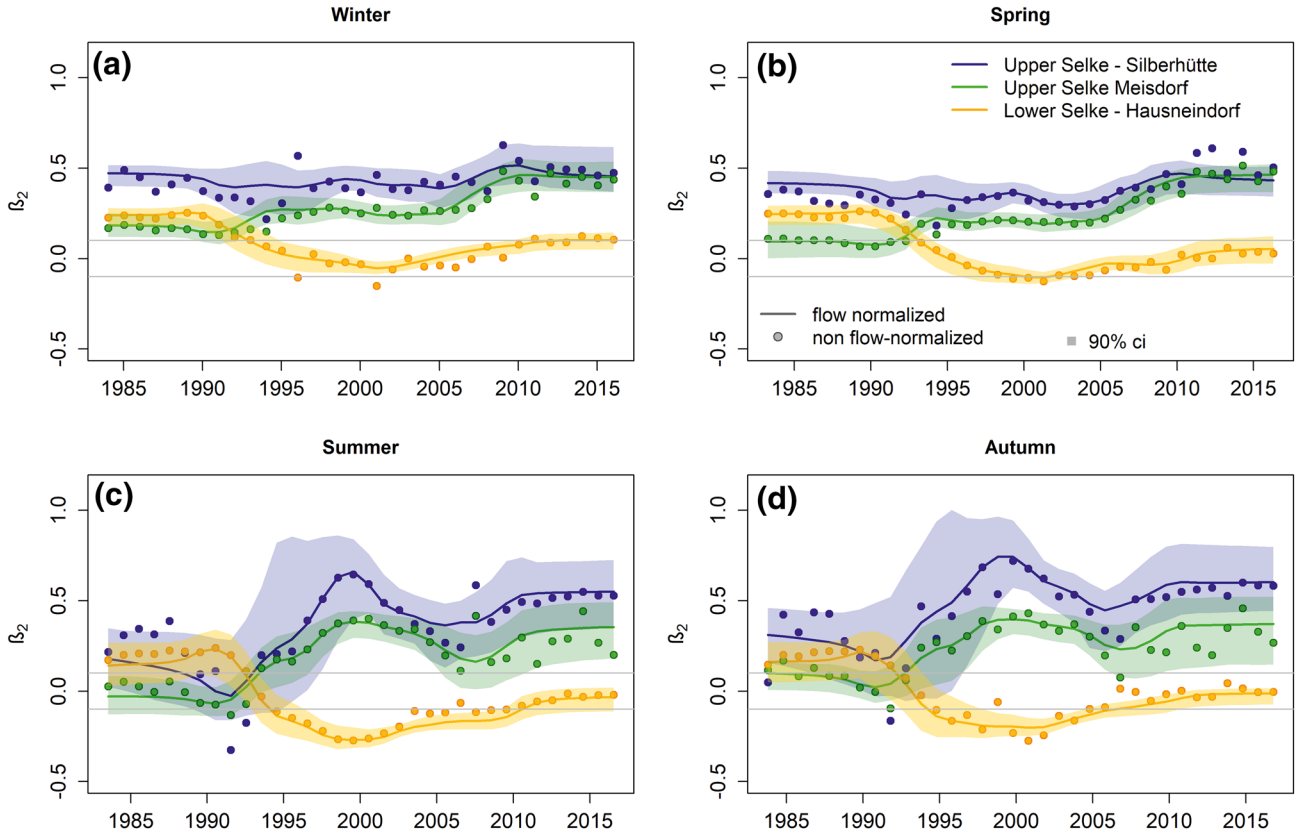

Figure 5. Long-term trends of the fitted parameter β_2, indicating the annual flow normalized (FN) and annual non-FN ln(concentration)–ln(discharge) relationship (*CQ* slope) from three nested subcatchments in the Selke catchment, separated for each season (a–d). Uncertainty bands in the subcatchment-specific color indicate the 90% confidence intervals from bootstrapping FN values. Horizontal gray lines delineate the border between chemostatic and chemodynamic nitrate transport.

3.4. Nitrate Retention and TTDs

Fitted TTDs as a transfer function between annual N input and annual FN nitrate concentrations show that TTs in the upper Selke were considerably shorter than those in the lower Selke (Table 2 and Figure. S3). Smaller modes and μ-values together with larger σ-values ($\sigma > 1$) in the upper Selke indicate a dominance of short TTs, whereas the higher mode and μ-value together with a lower σ-value ($\sigma < 1$) of the TTD in the lower Selke indicates a dominance of longer TTs and a considerably longer tailing. The convolution model was accurate for the upper Selke at Meisdorf ($R^2 = 0.92$) and acceptable for Silberhütte ($R^2 = 0.57$) as well as for the lower Selke ($R^2 = 0.40$; Table 2).

TTD-derived conservative N export over the period from 1983 to 2015 was higher than N input for this period (Table 2), because it integrated parts of the high N input from before 1983. We refer to the TTD-derived conservative N export that was not exported in the form of measured annual nitrate loads as the *missing N* (Van Meter et al., 2016; Table 2), which is either still in the catchments as legacy or removed via denitrification. All subcatchments of the Selke catchment showed a considerable percentage of *missing N* (80%–92%). This number is smallest for the upper Selke, especially for the upstream area draining to the gauge at Silberhütte, and largest for the lower Selke, with 10.8–11.5 kg ha^{-1} year^{-1} more N being missing than in the upper Selke.

3.5. Concentration–Discharge Relationships

Long-term *CQ* slopes in the upper Selke were positive, indicating chemodynamic nitrate export with an accretion pattern (Musolff et al., 2017), as was observed in seasonal (Figure 5) as well as in annual *CQ* slopes

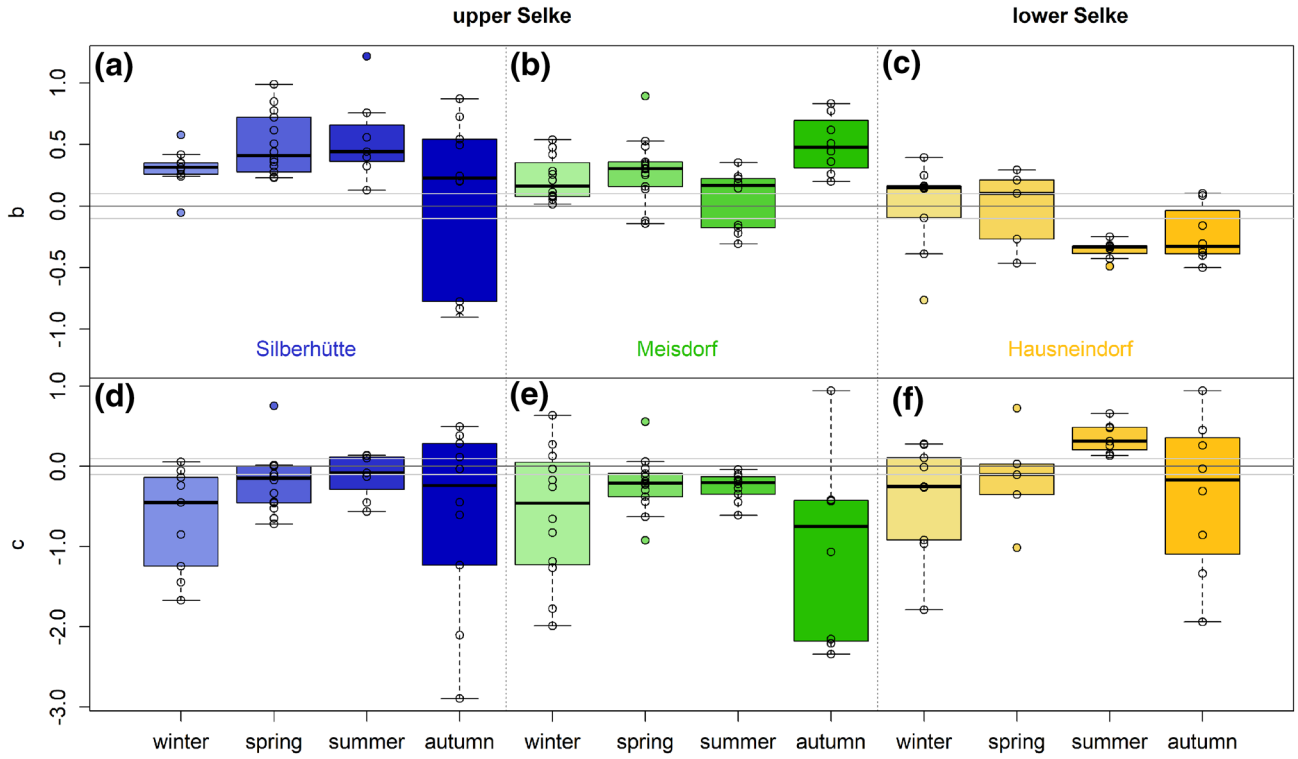

Figure 6. Boxplots of the event-specific fitted parameters *b* (*CQ* slope) and *c* (hysteresis) in Equation 2 with $R^2 > 0.5$. Parameters were separated by seasons and gauging stations within the Selke catchment, displayed from upstream (left) to downstream (right).

(Figure S2c). The only exception was for Meisdorf during LFSs between 1983 and 1990, where nitrate export was chemostatic with a *CQ* slope close to zero (Figures 5c and 5d). *CQ* slopes in Silberhütte were higher than the ones in Meisdorf, except for HFSs from 2010 on, for which *CQ* slopes were both around 0.45 (Figures 5a and 5b). During LFSs, *CQ* slopes in the upper Selke peaked in 1999 and, following a minimum around 2005, leveled out afterward. Uncertainty from sample estimates assessed via bootstrapping was highest for LFSs, but the generally positive *CQ* slopes beginning in 1990 were still evident (Figures 5c and 5d).

In contrast to the upper Selke, the export regime in the lower Selke changed significantly over time (Figure 5 and Figure S2c). *CQ* slopes in the lower Selke were positive between 1983 and 1990 for all seasons, indicating chemodynamic nitrate transport with accretion patterns. After 1990, *CQ* slopes decreased toward values around zero during HFSs (Figures 5a and 5b), which indicates chemostatic transport, and toward negative *CQ* slopes during LFSs (Figures 5c and 5d), which indicates chemodynamic nitrate export with a dilution pattern. Beginning around 2010, nitrate transport in the lower Selke was chemostatic during all seasons, with a tendency toward slightly higher *CQ* slopes during HFSs compared to during LFSs.

3.6. Storm Events

We identified a total of 200 storm events: 59 for Silberhütte (from 2013 to 2016), 72 for Meisdorf, and 69 for Hausneindorf (both from 2010 to 2016). Of all these events, 56% could be described adequately with the empirical formula which defines the hysteresis loop (Equation 2) with $R^2 > 0.5$. This is true for 40 events in Silberhütte, 44 in Meisdorf, and 29 in Hausneindorf, with at least seven events per season and gauge. Fitted parameters *b* and *c* for event-specific *CQ* slopes and hysteresis behavior of these events are displayed in Figure 6 and Figures S4 and S5. Upper Selke *CQ* slopes were dominantly positive, indicating chemodynamic nitrate export during storm events with an accretion pattern (Figures 6a and 6b). Some exceptions were found during November in Silberhütte, when some small events showed negative *CQ* slopes and caused a large variability in *CQ* slopes during this season (Table S1) and during summer in Meisdorf. Event-specific hysteresis in the upper Selke was dominantly counterclockwise, indicated by the negative parameter *c* (Figures 6d

and 6e). In contrast to the upper Selke, event-specific *CQ* slopes in the lower Selke were negative during LFSs, indicating chemodynamic nitrate transport with a dilution pattern (Figure 6c). During HFSs however, event-specific *CQ* slopes were dominantly positive, indicating an accretion pattern, similar to that found for the upper Selke. Hysteresis was clockwise during summer and dominantly counterclockwise during all other seasons, again similar to the situation in the upper Selke. For all three subcatchments, variability in hysteresis behavior was most pronounced during autumn. When looking at all identified events—regardless of their R^2 (Figures S4 and S5)—the described patterns in *CQ* slopes and hysteresis stayed evident, with the only exception being that *CQ* slopes in the lower Selke during spring were dominantly around zero or negative.

4. Discussion

4.1. Long-Term Trends in Nitrate Export

The nested catchment structure provided an ideal setting for analyzing the contribution of different subcatchments to nitrate export measured at the catchment outlet. This structure enabled us to calculate subcatchment-specific TTDs which revealed distinct time scales in the response of riverine nitrate export to N input within one mesoscale catchment. In the mountainous upper Selke, TTDs had their mode after 3 years, indicating a dominance of short TTs, while in the agriculturally dominated lower Selke, the TTD showed a peak after 12 years and a considerably longer tailing (Table 2). This difference can be explained mainly by a difference in hydrological TTs caused by a lower storage capacity (shallow soils and relatively impermeable geology) in the upper Selke, compared to the lower Selke (Haitjema, 1995). Consequently, N input in the upper Selke is transported rapidly to the stream network, and instream nitrate concentrations respond quickly to changes in N input, while in the lower Selke, N input is transported far more slowly and the response of nitrate concentrations to changes in N input is delayed by more than a decade. Long-term persistence of nitrate pollution is therefore more an issue in the lower Selke than in the upper Selke.

The subcatchment-specific differences in TTDs, furthermore, help to explain the different long-term trends in nitrate concentrations, loads, and *CQ* slopes (Figures 3–5). The rapid response of instream nitrate concentrations to changes in N input explains the decrease of nitrate concentrations and loads after 1990 in the upper Selke as an immediate consequence of the drastic decrease in N inputs (Figure 2) due to the German reunification and the associated break down of intensive agriculture. Our finding of short TTs in the upper Selke is in agreement with reported TTs from a small headwater catchment in the upper Selke (J. Yang et al., 2018) and with studies in other responsive headwater catchments for which comparably short TTs were reported (e.g., Hrachowitz et al., 2009; Soulsby et al., 2015). However, the increase in nitrate concentrations and loads during HFSs beginning in 2000 cannot be explained by TTDs and N input, because no pronounced increase of N input occurred around that time. One possible explanation could be an increase of distant nitrate sources that become connected to the stream with higher soil moisture content during HFSs and consequently more active flow path. Reasons for this might be local changes in agricultural practices, forest management, or land use arrangement, which were not accounted for in the county-based N input data. For example, spruce forests of the Harz Mountains were subjected to increased bark beetle attacks as a likely consequence of increasing temperatures (Lindner et al., 2010; Overbeck & Schmidt, 2012). The consequent die-back of trees could have caused changes in the N-balance of forest ecosystems in the upper Selke (Huber, 2005; Mikkelson et al., 2013).

In view of the large TTs in the lower Selke, we argue that the increase in N input before 1976 caused the increase in nitrate concentrations around 1990, while the decrease in N input that occurred in 1990 impacted riverine nitrate concentrations about a decade later (Figures 3 and 4, Figure S3). However, there is considerable uncertainty in the comparison between N input and export dynamics in the lower Selke, as suggested by the lower R^2 of the TTD (Table 2). Larger catchments with different land use types such as agriculture and urban areas are often exposed to multiple nitrate sources (Caraco & Cole, 1999; Silva et al., 2002). Hence, the observed dynamics in the lower Selke, especially the two emerging peaks during LFSs around 1997 and 2010, are likely a mixture of delayed N input and additional direct influences from other nitrate sources. Two possible direct influences are (i) the activities around the mining pit close to the catchment outlet and (ii) the starting operation of WWTPs around 1996/1997. Water was pumped from the mining pit into the Selke River before 1991 and after 2009, while water was diverted from the river into the

pit between 1998 and 2009. The few available grab samples of nitrate concentration at the outlet of the filled mining pit (mainly after 2009, Figure S6) suggest a temporal dilution of riverine nitrate concentrations and it remains unclear how these activities changed groundwater gaining or losing conditions in the Selke River itself (Figure S6). We showed not only that WWTPs generally have a small impact on nitrate concentrations (Figure 2) but also that their impact is highest during LFSs. Hence, it is possible that temporal changes that cannot be accounted for by the resolution of our WWTP data contributed to the decrease in nitrate concentrations around 1997.

In summary, although the decline in nitrate concentrations in the lower Selke is generally a good sign for improved water quality, its driving forces are related to considerable uncertainty. Nitrate concentrations might have decreased as a delayed response to the decrease in N input in 1990 or due to other more direct influences such as the nearby mining pit. We suggest that a combination of all these processes was responsible for the observed concentration dynamics.

4.2. Long-Term Trends in Concentration–Discharge Relationships

CQ slopes in the upper Selke showed an overall consistent picture of chemodynamic accretion patterns in nitrate export (Figure 5). Low *CQ* slopes during LFSs before 1990 might indicate N saturation of the catchments due to the high agricultural N input during this time (Figure 2). *CQ* slopes increased toward chemodynamic accretion patterns after the decrease of N inputs in 1990, suggesting that the landscape is becoming less saturated and that there is more heterogeneity in nitrate sources and pathways; however, nitrate export was still transport limited. In 2000, *CQ* slopes during LFSs decreased but maintained chemodynamic accretion patterns as an indication of transport limitation. We argue that the more dynamic *CQ* slopes during LFSs (compared to HFSs) are likely linked to seasonal conditions such as decreased hydrologic connectivity and a greater biological N demand.

CQ slopes in the lower Selke changed from (i) an accretion pattern before 1990 to (ii) dilution in LFSs and chemostasis in HFSs and finally toward (iii) chemostatic nitrate export during all seasons in recent years (Figure 5). A very similar dynamic of *CQ* slopes was reported by Ehrhardt et al. (2019) for a nearby mesoscale catchment. They explained this by the vertical stratification of nitrate storage in the subsurface as a consequence of the downward transport of nitrate with time (Dupas et al., 2016) and different active flow paths during HFSs and LFSs. During LFSs, *Q* is dominated by base flow originating from deeper groundwater, whereas shallower subsurface flow paths which access a younger fraction of groundwater are activated during HFSs (Ehrhardt et al., 2019; Musolff et al., 2016). As N input gradually increased until 1976, deeper groundwater in the lower Selke still showed lower nitrate concentrations than shallow groundwater in the first years of our time series. Consequently, nitrate concentrations during low-flow conditions were lower than concentrations during high flow, leading to the observed accretion pattern. After the German reunification in 1990, N input drastically decreased leading to a decrease of nitrate concentrations in shallow groundwater and higher concentrations in deeper groundwater due to the downward percolation of the high N inputs from before 1990 (Figure 2). Consequently, nitrate concentrations in the lower Selke were higher during low-flow conditions than during high-flow conditions, leading to the observed dilution pattern. Another reasonable explanation for the dilution pattern is the impact from upper Selke nitrate export. Due to the shorter TTs and the consequently faster transport of N in the upper Selke, long-term trends in riverine nitrate concentrations showed an immediate decrease after 1990, while concentrations still increased in the lower Selke. These diverging long-term trends were especially pronounced during LFSs (Figures 3c and 3d). Lower nitrate concentrations from the upper Selke during LFSs could therefore have diluted the higher nitrate concentrations downstream, leading to the observed dilution pattern in *CQ* slopes in the lower Selke (Figures 5c, 5d, and S2c). Most plausibly, a mixture of both vertical layering of groundwater nitrate concentrations and the impact of the upper Selke led to the observed dilution pattern. In recent years, chemostatic nitrate export during all seasons developed in the lower Selke, likely due to a mixture of both vertical equilibration of groundwater nitrate concentrations after a prolonged period of stable N inputs (Figure 2; Dupas et al., 2016; Ehrhardt et al., 2019) and a less pronounced dilution effect from the upper Selke due to converging nitrate concentration levels between the subcatchments (Figure 3).

Similarly to Ehrhardt et al. (2019), we were able to show that *CQ* relationships transitionally shift with changes in N input and further that these changes can be different between seasons. Thus, chemostatic ni-

trate export is an indication not exclusively for intensive agriculture but also for homogenously distributed N stores, both vertically in the subsurface and between different subcatchments. In fact, chemodynamic export at the catchment outlet can also indicate "not equilibrated systems," where changes in N input have not yet propagated through the whole system, causing a vertical layering of nitrate concentrations in the subsurface and/or diverging nitrate concentration between subcatchments due to different subcatchment-specific TTDs. Defining one unique *CQ* slope for nitrate concentrations at the catchment outlet across longer time series and seasons can be misleading, as it may integrates input and mobilization patterns as well as transport times that are not necessarily the same over space and time (Figure S7). For example, a temporal transition from accretion patterns toward dilution—as observed in the lower Selke during LFSs from 1990 to 2000—might be interpreted as constantly chemostatic if these long-term temporal changes and for seasonal differences are not taken into account.

4.3. N Legacies and Potential Denitrification

The largest proportion of N export that should have been exported according to TTDs is "missing." Only 15.4% and 8.0% of the estimated N export derived from conservative TTDs were actually exported as measured nitrate loads, which translates into 34.8 kg N ha^{-1} $year^{-1}$ and 46.3 kg N ha^{-1} $year^{-1}$ of *missing N* (Table 2). This is likely evidence of considerable N retention in both subcatchments, especially in the lower Selke.

The relatively constant *CQ* slopes in the upper Selke indicate biogeochemical legacies, while short TTs suggest a fast turnover of hydrological legacies that prevent a similar vertical stratification and associated heterogeneity in the belowground N storage as discussed for the lower Selke. The observed chemodynamic accretion pattern and the pronounced seasonality also indicate that N sources are stored either in the shallower zones of the subsurface or in the more distant zones to the stream network, which could both be partially activated during high-flow conditions such as storm events during winter. This explanation is supported by J. Yang et al. (2018), who proposed that an expansion of discharge generating zones during high-flow conditions in a small headwater catchment in the upper Selke enables the mobilization of additional N sources. In contrast, long TTs and the shifts in *CQ* relationships in the lower Selke indicate the presence of considerable hydrological legacies, as nitrate export patterns are driven by the seasonal activation of different N source zones with different ages, as discussed above (Ehrhardt et al., 2019).

Denitrification is the only process leading to permanent nitrate removal within the catchment. It accounts for a part of the *missing N* and prevents it from being stored in the catchment (Seitzinger et al., 2006). Kuhr et al. (2014) calculated average denitrification rates for soils in Saxony-Anhalt using the process-based DENUZ transport model (Köhne & Wendland, 1992; Kunkel & Wendland, 2006) and showed that denitrification rates in the unsaturated zone in and around the Selke catchment are low to very low (9–13 kg ha^{-1} $year^{-1}$), which is considerably lower than the rates of *missing N* for the Selke catchment mentioned above (Table 2). Even assuming the upper range denitrification rate, *missing N* would still be >20 kg N ha^{-1} $year^{-1}$ in the upper and >30 kg N ha^{-1} $year^{-1}$ in the lower Selke.

According to a recent study from Hannappel et al. (2018), the potential for denitrification in the groundwater is largely depleted in Saxony-Anhalt. Hannappel et al. compared N input with nitrate concentrations in the groundwater and searched for hydrogeochemical evidence of ongoing denitrification (redox status, increase in hydrogencarbonate or sulfate). Of the seven observation wells within the Selke catchment, only one (located in the upper Selke) showed evidence of ongoing denitrification. Hence, denitrification in the groundwater likely removed a part of N input in the upper Selke. However, of all observation wells in Saxony-Anhalt located in a similar geologic setting as the upper Selke (Palaeozoic), fewer than 5% showed evidence of ongoing denitrification. This is a warning sign for the upper Selke, indicating that essential electron donors such as pyrite for autolithotrophic denitrification have been largely consumed or might become depleted in the near future. None of the observation wells showed a potential for denitrification in groundwater in the lower Selke (Hannappel et al., 2018). We therefore argue that denitrification in groundwater played only a minor role for the fate of N input in the lower Selke, an assumption which is in line with findings from Ehrhardt et al. (2019) made in a nearby mesoscale catchment. Nevertheless, there is evidence for significant denitrification in the riparian zones, especially during LFSs. Recent studies by Lutz et al. (2020) and Trauth et al. (2018) reported a removal by riparian denitrification of up to 12% of nitrate

from groundwater entering the Selke River along a 2-km section downstream of Meisdorf. Additionally, a stable isotope study by Mueller et al. (2016) in the Bode catchment (which includes the Selke catchment) found evidence for significant denitrification in the stream beds during LFSs, whereas denitrification in the groundwater was not evident, findings which are in line with those of Hannappel et al. (2018). The studies agree that riparian zone and stream bed denitrification are more likely to occur in the downstream part of the river where flow velocities are reduced, which suggests that this type of denitrification might be an important process for the lower but not evidently for the upper Selke.

Assimilatory uptake in the stream is another important process in nitrate export dynamics: it could, according to Rode et al. (2016), have removed around 5% of nitrate in the upper Selke and 13% in the lower Selke. Nevertheless, only a small percentage of nitrate uptake is the permanent removal via denitrification. Hence, we suggest that N uptake in the stream only accounts for a small percentage of the *missing N*. Moreover, following the argument of Ehrhardt et al. (2019), the change in seasonal patterns in the lower Selke and the high nitrate concentrations in LFSs around 1997 (Figures 3c and 3d) indicate that assimilatory uptake was not a key process in causing the observed nitrate export patterns at longer time scales, as this would imply a more steady seasonality.

In summary, a large proportion of N was not exported from the Selke River and is therefore missing. It is unlikely that denitrification alone is responsible for all *missing N*, which means that part of it was stored as biogeochemical and hydrological legacies in both parts of the catchment. We see an indication for biogeochemical legacies in the upper Selke, whereas long TTs and deeper aquifers indicated an important contribution of hydrological legacies in the lower Selke. As N input and the percentage of *missing N* in the lower Selke was higher, extensive N legacies and especially long-term nitrate pollution are more of an issue in the agriculturally dominated lowland parts of the catchment than in the mountainous upstream part. Groundwater-dominated catchments like the lower Selke are generally more prone to hydrological legacies (Van Meter & Basu, 2017). As these (sub)catchments are typically associated with agricultural land use, they are most prone to developing nitrate legacies.

4.4. Seasonality in Nitrate Export

The contribution of different subcatchments to nitrate export in the Selke catchment was highly seasonal, with significant differences between HFSs and LFSs. While the upper Selke dominated nitrate export during HFSs, the lower Selke dominated during LFSs. This seasonal shift in the dominant subcatchment for nitrate export was driven by the seasonally different dynamics of mobilization and transport in the different subcatchments.

Nitrate concentrations in the upper Selke showed a pronounced seasonality, with high concentrations during HFSs and low concentrations during LFSs. This dynamic might have several reasons, such as an increased N demand of the ecosystems during warmer temperatures (Rode et al., 2016), a flushing of limited surficial N sources with peak snowmelt (Pellerin et al., 2012), and a higher hydrological connectivity due to an increased soil moisture content during HFSs (J. Yang et al., 2018). Especially, the last point is also reflected by the positive *CQ* slopes in the upper Selke, which indicate *CQ* a chemodynamic-accretion pattern (Figure 5). This accretion pattern can be explained by the activation of additional N sources with efficient transport to the stream during wet conditions (J. Yang et al., 2018). In contrast to chemostatic patterns, N sources in a chemodynamic-accretion pattern are not uniformly distributed. Instead, distinct sources become activated during certain flow conditions. Therefore, accretion patterns hint at patchy N sources and spatially limited N legacies. This might be a common situation in mountainous and forest-dominated upstream catchments which include only patches of agriculture or other relevant N sources. The consequent increase in nitrate concentrations during high flows and HFSs can cause high nitrate loads, as observed in the upper Selke and other forest-dominated catchments (Seybold et al., 2019). Although it is known that upstream catchments can have an important role for nutrient transport (Alexander et al., 2007; Goodridge & Melack, 2012), the contribution from the upper Selke to 78.4% of overall nitrate loads during winter and 64% annually was unexpectedly high, given the fact that the upper Selke comprises only 17% of the catchment's agricultural area and contributed on average only 37% of total N input. We explain this disproportional contribution to nitrate loads by (i) the high nitrate concentrations during HFSs which indicate an

additional activation of N sources with higher *Q* as reflected by the described accretion pattern and by (ii) a disproportional contribution to *Q* from the upper Selke, which is typical for upstream catchments (Alexander et al., 2007; Dupas et al., 2019) and might be enhanced by snowmelt during HFSs due to the higher elevations in the upper Selke (Table 1).

Nitrate concentrations in the lower Selke generally showed a less pronounced seasonality compared to the upper Selke, especially since 2010, when nitrate export became chemostatic during all seasons (Figure 5). Chemostatic export was often found for catchments like the lower Selke which are dominated by agricultural land use, indicating a considerable amount of nitrate legacy stores (Basu et al., 2010, 2011) and a prolonged period of relatively stable N inputs (Ehrhardt et al., 2019). Due to the decreasing contribution from the upper Selke during LFSs and base flow conditions, the relatively constant nitrate input (around 3.1 mg L^{-1}) in the lower Selke kept nitrate concentrations high during these periods and consequently dominated nitrate export under dry conditions when surface waters are subject to an increased risk of eutrophication and a consequent loss of aquatic biodiversity (Whitehead et al., 2009). Another factor that could have caused high or nondecreasing nitrate concentrations during LFSs is the constant contribution from WWTPs that have a relatively higher impact when stream *Q* is low. However, their overall contribution to nitrate export in the lower Selke was low, even during LFSs (6.2%–9.4%), and the dilution pattern during events indicates no significant impact from rainwater overflow basins. Outflow from WWTPs were therefore certainly not the dominant driving force for elevated nitrate concentrations during LFSs.

In conclusion, the pronounced seasonality in the upper Selke leads to a dominance of nitrate export during HFSs and a disproportional contribution to annual nitrate loads. During LFSs, the contribution to nitrate export from the upper Selke is small and consequently the relatively constant nitrate export from the lower Selke dominates. The integrated signal of nitrate export patterns, measured at the catchment outlet, is not a constant mixture of subcatchment-specific signals but reflects a seasonal dominance of different subcatchments. These results emphasize the importance of analyzing seasonal dynamics in different parts of larger catchments in order to identify the patterns of most dominant N sources at different times of the year (under different hydrological conditions) and thus the temporal interplay between different high-risk zones for N pollution.

4.5. Event Dynamics and Their Seasonality

To examine the integrated signal of nitrate export across time scales, we analyzed not only long-term trends and seasonal patterns but also the *CQ* slopes and hysteresis behavior during single events. Because high-frequency data for event analysis were available between 2010 and 2016, we could directly compare long-term trends and event dynamics during this common period. Event-specific as well as long-term *CQ* slopes in the upper Selke were dominantly positive, indicating chemodynamic export with an accretion pattern that is time scale independent (Figures 6a and 6b). Large storm events can therefore mobilize and transport large amounts of nitrate and contribute disproportionally to annual nitrate loads. The counterclockwise hysteresis found for most events (Figures 6d and 6e) indicates that N sources are mobilized with a delay to *Q*, which can be explained by distant N sources and higher nitrate concentrations in riparian floodplain aquifers that dominate the falling limb of event *Q* (Rose et al., 2018; Sawyer et al., 2014).

In the lower Selke, long-term *CQ* slopes between 2010 and 2016 showed a chemostatic pattern, whereas event-specific *CQ* slopes were more dynamic (Figure 5; Figure 6c). The event-specific dilution patterns (negative *CQ* slopes) in LFSs in the lower Selke can be explained by lower nitrate concentrations from the upper Selke (Figures 3c and 3d) that diluted lower Selke nitrate concentrations. Additionally, they might be caused by a direct dilution from shallow flow paths with reduced nitrate concentrations due to an elevated N demand by agricultural crops during summer and early fall that were activated during events and diluted the more highly concentrated base flow. During winter, event-specific *CQ* slopes in the lower Selke became dominantly positive (Figure 6c), indicating a chemodynamic export with the same accretion pattern as in the upper Selke. It is also during recent winters that nitrate concentrations from the upper Selke were similarly high as the nitrate concentrations in the lower Selke (Figure 3a). It is therefore reasonable to assume that higher nitrate concentrations from the upper Selke during storm events also caused an increase in concentrations in the lower Selke and led to the described accretion pattern during winter events. The observed counterclockwise hysteresis during winter confirms this assumption, because it was also observed in the upper Selke and indicates more distant nitrate sources (Musolff et al., 2017) which, in this case, might

represent the impact from the upper Selke. For both dilution from spring to autumn and accretion during winter, the event dynamics in the lower Selke are considerably influenced by the upper Selke nitrate export.

Event-specific *CQ* slopes estimated at the catchment outlet (lower Selke) are in accordance with findings from Bowes et al. (2015), who reported a dominance of dilution patterns during storm events at the outlet of a mesoscale catchment that integrates different types of land use (39% agriculture, 27% grassland, and 23% woodland). Similarly to the findings in our study, the only accretion pattern was observed during winter. Bowes et al. (2015) related this accretion pattern to an additional mobilization of distant agricultural N sources, which are comparable to our findings with respect to mobilization from the upper Selke. Furthermore, they argued that diffuse N sources become depleted throughout large storm events in winter and spring, which might also be the case (to a lesser extend) in the upper Selke catchment and could explain its lower export levels of nitrate during spring compared to winter (Figures 3a, 3b, 4a, and 4b). Moreover, Dupas et al. (2016) found a similar dilution pattern during most storm events at the outlet of a mesoscale catchment in Thuringia (Germany), whereas long-term trends increasingly showed chemostasis, as observed in the lower Selke. These comparisons show that nitrate export patterns observed at the Selke catchment are not an isolated phenomenon. Taking advantage of the nested catchment study design in the Selke catchment that allowed us to identify subcatchment-specific contributions, we suggest that the contrast between long-term and event-specific *CQ* slopes in the lower Selke reflects the upstream subcatchment export patterns and therefore serves as an indicator to disentangle subcatchment-specific contributions to nitrate export and its dynamics.

4.6. Conceptual Framework and Implications for Management

A key objective of this study was to analyze how different nested subcatchments contribute to the integrated signal of nitrate concentrations, loads, and *CQ* relationships at the outlet of a mesoscale catchment. While upstream subcatchments are known to have a disproportional impact on nutrient transport (e.g., Alexander et al., 2007; Dodds & Oakes, 2008; Goodridge & Melack, 2012), agricultural areas (which are more likely to occur in downstream lowlands) are known to be a major source of nitrate pollution (e.g., Padilla et al., 2018; Strebel et al., 1989). The available long-term and high-frequency data for three nested catchments within the Selke catchment enabled us to disentangle these contrasting drivers of nitrate export and allowed a detailed analysis of the relative impact of more mountainous upstream subcatchments (upper Selke) versus more intensively cultivated downstream lowlands (lower Selke) across time scales. The general findings, summarized in Figure 7, illustrate that TTs for nitrate in the upper Selke were relatively short (Figure 7a) and that transport patterns were quite dynamic, with nitrate concentration increasing with *Q* (Figures 7b and 7c). These dynamics led to temporally elevated nitrate concentrations during HFSs and events and a disproportional contribution to annual nitrate loads, which are both relatively short-term impacts. In contrast, the lower Selke showed long TTs (Figure 7a) and a less dynamic export behavior with relatively constant nitrate concentrations (Figures 7b and 7c). Due to the long TTs, the imbalance between TTD-derived conservative N export and measured N export and the low potential for denitrification, legacy stores in the downstream part are expected to be significant. Consequently, nitrate pollution in the lower Selke is a rather long-term and persistent problem that will likely impact nitrate exports for years to come, dominantly during LFSs and base flow conditions. This differentiation between a more mountainous upper part of a catchment and an agriculturally dominated lowland part is very common for mesoscale catchments in temperate climates (e.g., Krause et al., 2006; Montzka et al., 2008); hence our findings have far reaching consequences for the management of nitrate pollution in such catchments.

Water quality managers should be aware of these potential differences between subcatchments. If the aim is to reduce high nitrate loads, the focus must be on the upstream subcatchments with short TTDs and dynamic transport patterns. As nitrate concentrations are especially high during winter and spring, an application of catch crops during these seasons is a promising measure to reduce nitrate leaching (Askegaard et al., 2005; Constantin et al., 2010; McLenaghen et al., 1996). Furthermore, large buffer strips (>50 m) can decrease connectivity between agricultural fields and the stream network (Mayer et al., 2005). Unfortunately, high N loading via atmospheric deposition, as apparently occurs in the Harz Mountains (Kuhr et al., 2014), cannot be addressed locally but requires a large-scale reduction of fertilizer application and fossil fuel combustion. Nevertheless, a substantial reduction of N surplus from agriculture and measures to decrease nitrate leaching are believed to have the potential to significantly and relatively quickly reduce nitrate export to the streams, as the riverine concentration decrease after 1990 suggests.

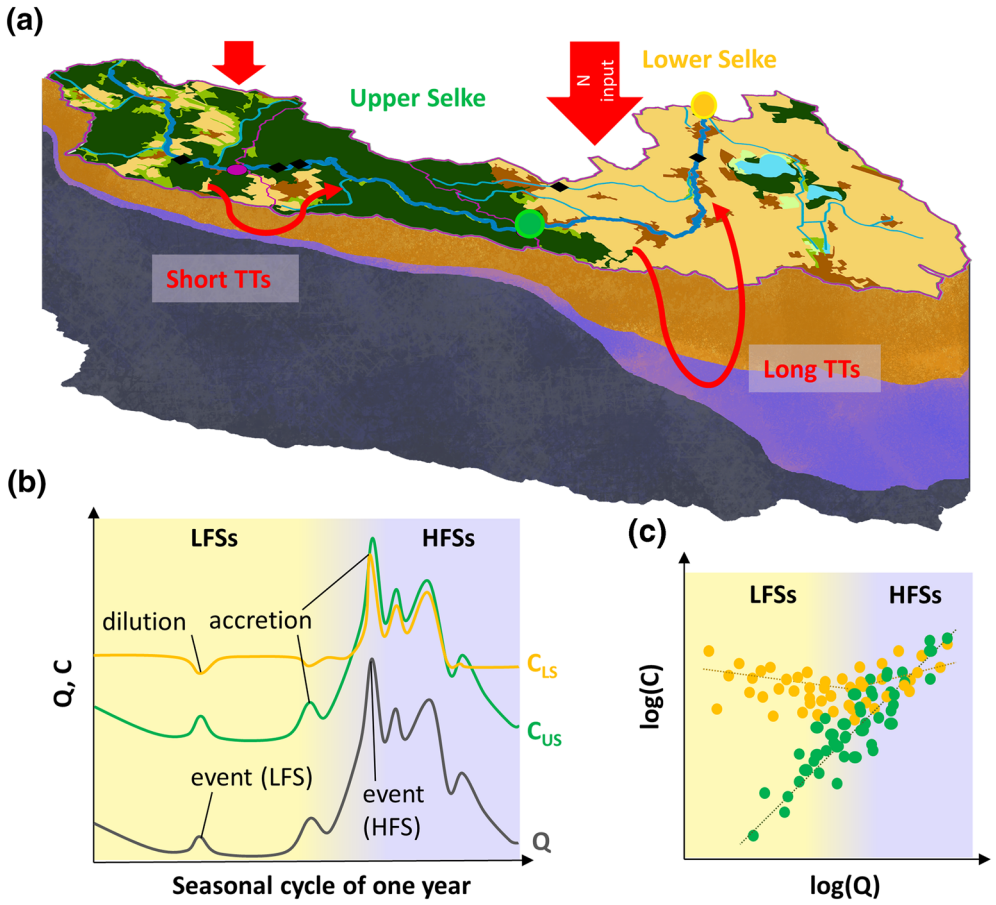

Figure 7. Conceptual framework explaining the subcatchment-specific contribution of the upper Selke (green) and the lower Selke (yellow) to nitrate export from the Selke catchment during low-flow seasons (LFSs, yellow background in (b) and (c)) and high-flow seasons (HFSs, blue background in (b) and (c)). Note that nitrate export from the lower Selke is always an integrated signal from the entire catchment. (a) The Selke catchment divided into the upper Selke (green circle) and the lower Selke (yellow circle) with its land use, its relative N input (not true to scale), and apparent travel times of nitrate (TTs). (b) Seasonal and event dynamics of nitrate concentrations (*C* with indexed US and LS representing the upper and lower Selke) and (c) the long-term *CQ* relationships. Note that long-term *CQ* relationships, as depicted in (c), do not account for temporal shifts but represent the integrated signal.

If the aim is to reduce low-flow nitrate concentrations to protect drinking water resources and aquatic ecosystems on the long-term, lowland areas with extensive agricultural land use and long TTs need to be the target for remediation measures. However, long TTs and legacy stores will impede a quick success of nitrate reduction measures and will likely affect drinking water quality and low-flow instream concentrations for years to come. For such groundwater-dominated systems, long-term management strategies to reduce fertilizer application on a large scale will be needed to effectively address nitrate pollution (Bieroza et al., 2018; Ehrhardt et al., 2019).

In any case, to address short-term *and* long-term nitrate pollution, water quality managers should focus neither solely on upstream areas of catchments nor solely on the lowland areas where most of the agricultural land use typically occurs. Instead, they need to integrate all characteristic landscape units and their interaction.

5. Conclusions

A key goal of this study was to characterize the spatial variability in nitrate export dynamics across nested subcatchments and to disentangle their respective contributions to the integrated signal of nitrate export at the catchment outlet. Taking advantage of a comprehensive data set that includes long-

term and high-frequency data from three nested subcatchments in the Selke catchment, we were able to show that subcatchments can have very different nitrate export dynamics that lead to seasonally different subcatchment contributions to nitrate concentrations and loads. The mountainous upstream part of the catchment (here the upper Selke) transports temporally elevated nitrate concentrations during HFSs and events and therefore has a disproportionally high contribution to nitrate loads. This imbalance underlines the important role of upstream subcatchments when considering effective measures to reduce nitrate pollution. Hence, nitrate export from hydrologically responsive upstream catchments can be a serious threat to water quality, especially with respect to exported loads. At the same time, short TTs emphasize a fast response to changes in N input and dedicated mitigation measures are likely to show effects relatively quickly. In contrast, lowland subcatchments with long TTs and a dominance of agricultural land use (here the lower Selke) pose a long-term and persistent problem in terms of nitrate pollution; the quality of drinking water can be threatened for decades. Nitrate export from these subcatchments is relatively steady and dominates during LFSs and base flow conditions. Its impact on nitrate concentrations during HFSs and events and especially on nitrate loads, however, might be overestimated if the impact from upstream subcatchments is not taken into consideration. We do not aim at prioritizing individual measures to reduce nitrate pollution between subcatchments, but we emphasize the importance of subcatchment-specific characteristics in order to place nitrate reduction measures most effectively and to assume realistic time scales for their success.

We could further show that *CQ* relationships for nitrate concentrations can change as a reaction to changes in N input. Whereas chemodynamic patterns can indicate "not equilibrated systems" that are still in transition toward a new equilibrium, chemostasis can indicate homogenously distributed N sources (both vertically in the subsurface and between subcatchments) after a prolonged period of stable N inputs. To detect these changes, it is crucial to account for temporal changes and seasonality in *CQ* relationships. Furthermore, we found that the combined analysis of long-term trends and event-scale *CQ* slopes is a promising approach to disentangle the impact from subcatchments on nitrate export at the catchment outlet, as it can reveal short-term impacts from the more dynamic upstream catchment export which is relevant for load estimations and a more precise detection of N sources. Examining the whole range of time scales—from long-term trends to the event scale—is therefore crucial in order to be able to assess the full range of subcatchment impacts on nitrate export, as the times and time scales relevant for nitrate export can vary substantially between subcatchments.

Findings from this study should be further tested by applying our (or similar) approaches to other mesoscale catchments with different characteristics and in different settings. Including the knowledge gained from such studies on subcatchment contributions to nitrate export into spatially distributed water quality models would eventually lead to more precise projections and, in turn, to more robust management strategies for water quality.

Data Availability Statement

Supplementary figures and tables are available as Supplementary Information. Data sets on (i) FN and non-FN nitrate concentrations, loads, and *CQ* slopes; (ii) N input; and (iii) event characteristics are available under: https://doi.org/10.4211/hs.c3ea08faa88a46a4a3ce596a09686198

Raw data on discharge and water quality are freely available on the website of the State Office of Flood Protection and Water Quality of Saxony-Anhalt (LHW), from gldweb.dhi-wasy.com/gld-portal/

High-frequency data of nitrate concentrations are archived in the TERENO data base and are available upon request through the TERENO-Portal (www.tereno.net/ddp).

Atmospheric deposition data can be accessed on the website of the Meteorological Synthesizing Centre—West (MSC-W) of the European Monitoring and Evaluation Programme (EMEP) (http://emep.int/mscw/index_mscw.html, Norwegian Meteorological Institute, 2017), which is assigned to the Meteorological Institute of BNorway (MET Norway).

The raw meteorological data sets can be freely obtained from the German Weather Service (DWD) and gridded products based on Zink et al. (2017) from https://www.ufz.de/index.php?en=41160

Acknowledgments
Funding for this study was provided by the DFG collaborative research center (SFB) 1253 "CAMPOS" as well as by the Helmholtz Research Program, Integrated Project "Water and Matter Flux Dynamics in Catchments." R.K. and M.W. acknowledge the partial funding from the Initiative and Networking Fund of the Helmholtz Association through the project Advanced Earth System Modeling Capacity (ESM) (www.esm-project.net). The authors cordially thank the State Office of Flood Protection and Water Quality of Saxony-Anhalt (LHW) for providing discharge and nitrate concentration data and to the Ministry of Environment, Agriculture and Energy Saxony-Anhalt (MULE) for the provision of WWTP data. Furthermore, the authors would like to thank Martin Bach from the University of Gießen for supplying N input data from agricultural areas and the MET Norway for supplying data to simulate atmospheric deposition. The authors thank Michael Rode for the provision of high-frequency data from TERENO observational facilities and the German Meteorological Service for the provision of meteorological data sets. The authors thank Florian Schnabel for brainstorming on the conceptual framework, Kathrin Kuehnhammer and Samuel Mayer for their input to R codes for base flow separation, and Frederic Bartlett for correction reading. Additionally, we thank the three anonymous reviewers for their valuable and constructive feedback that helped to improve the original manuscript.

References

Alexander, R. B., Boyer, E. W., Smith, R. A., Schwarz, G. E., & Moore, R. B. (2007). The role of headwater streams in downstream water quality 1. *JAWRA Journal of the American Water Resources Association*, *43*(1), 41–59. https://doi.org/10.1111/j.1752-1688.2007.00005.x

Askegaard, M., Olesen, J. E., & Kristensen, K. (2005). Nitrate leaching from organic arable crop rotations: Effects of location, manure and catch crop. *Soil Use & Management*, *21*(2), 181–188. https://doi.org/10.1111/j.1475-2743.2005.tb00123.x

Bach, M., Breuer, L., Frede, H.-G., Huisman, J. A., & Otte, A. (2006). Accuracy and congruency of three different digital land-use maps. *Landscape and Urban Planning*, *78*(4), 289–299. https://doi.org/10.1016/j.landurbplan.2005.09.004

Bach, M., & Frede, H.-G. (1998). Agricultural nitrogen, phosphorus and potassium balances in Germany—Methodology and trends 1970 to 1995. *Zeitschrift für Pflanzenernährung und Bodenkunde*, *161*(4), 385–393. https://doi.org/10.1002/jpln.1998.3581610406

Bartnicky, J., & Benedictow, A. (2017). Atmospheric deposition of nitrogen to OSPAR convention waters in the period 1995–2014. EMEP MSC-W Report for OSPAR EMEP/MSC-W Technical Report.

Bartnicky, J., & Fagerli, H. (2004). Atmospheric nitrogen in the OSPAR convention area in the period 1990–2004. Summary Report for the OSPAR convention (EMEP Technical Report MSC-W 4/2006). Oslo, Norway: Norwegian Meteorological Institute.

Basu, N. B., Destouni, G., Jawitz, J. W., Thompson, S. E., Loukinova, N. V., Darracq, A., et al. (2010). Nutrient loads exported from managed catchments reveal emergent biogeochemical stationarity. *Geophysical Research Letters*, *37*, L23404. https://doi.org/10.1029/2010GL045168

Basu, N. B., Thompson, S. E., & Rao, P. S. C. (2011). Hydrologic and biogeochemical functioning of intensively managed catchments: A synthesis of top-down analyses. *Water Resources Research*, *47*, W00J15. https://doi.org/10.1029/2011WR010800

Behrendt, H., Huber, P., Kornmilch, M., Opitz, D., Schmoll, O., Scholz, G., & Uebe, R. (2000). (O.). Nutrient emissions into river basins of Germany. *Environmental Research of the Federal Ministry of the Environment, Nature Conservation and Nuclear Safety - Research Project Water - Research Report 296 25 515, UBA-FB 99-087/e*, *Texte*(23), 261

Bernal, S., Butturini, A., & Sabater, F. (2002). Variability of DOC and nitrate responses to storms in a small Mediterranean forested catchment. *Hydrology and Earth System Sciences Discussions*, *6*(6), 1031–1041.

Bieroza, M. Z., Heathwaite, A. L., Bechmann, M., Kyllmar, K., & Jordan, P. (2018). The concentration–discharge slope as a tool for water quality management. *The Science of the Total Environment*, *630*, 738–749. https://doi.org/10.1016/j.scitotenv.2018.02.256

Blöschl, G., Bierkens, M. F., Chambel, A., Cudennec, C., Destouni, G., Fiori, A., et al. (2019). Twenty-three unsolved problems in hydrology (UPH)—A community perspective. *Hydrological Sciences Journal*, *64*(10), 1141–1158. https://doi.org/10.1080/02626667.2019.1620507

Bouraoui, F., & Grizzetti, B. (2011). Long term change of nutrient concentrations of rivers discharging in European seas. *The Science of the Total Environment*, *409*(23), 4899–4916. https://doi.org/10.1016/j.scitotenv.2011.08.015

Bowes, M. J., Jarvie, H. P., Halliday, S. J., Skeffington, R. A., Wade, A. J., Loewenthal, M., et al. (2015). Characterising phosphorus and nitrate inputs to a rural river using high-frequency concentration–flow relationships. *The Science of the Total Environment*, *511*, 608–620. https://doi.org/10.1016/j.scitotenv.2014.12.086

Breuer, L., Vache, K. B., Julich, S., & Frede, H.-G. (2008). Current concepts in nitrogen dynamics for mesoscale catchments. *Hydrological Sciences Journal*, *53*(5), 1059–1074. https://doi.org/10.1623/hysj.53.5.1059

Burns, D. A., Pellerin, B. A., Miller, M. P., Capel, P. D., Tesoriero, A. J., & Duncan, J. M. (2019). Monitoring the riverine pulse: Applying high-frequency nitrate data to advance integrative understanding of biogeochemical and hydrological processes. *Wiley Interdisciplinary Reviews: Water*, *6*(4), e1348. https://doi.org/10.1002/wat2.1348

Camargo, J. A., & Alonso Á. (2006). Ecological and toxicological effects of inorganic nitrogen pollution in aquatic ecosystems: A global assessment. *Environment International*, *32*(6), 831–849. https://doi.org/10.1016/j.envint.2006.05.002

Caraco, N. F., & Cole, J. J. (1999). Human impact on nitrate export: An analysis using major world rivers. *Ambio*, *28*(2), 167–170.

Cleveland, C. C., Townsend, A. R., Schimel, D. S., Fisher, H., Howarth, R. W., Hedin, L. O., et al. (1999). Global patterns of terrestrial biological nitrogen (N_2) fixation in natural ecosystems. *Global Biogeochemical Cycles*, *13*(2), 623–645. https://doi.org/10.1029/1999GB900014

Constantin, J., Mary, B., Laurent, F., Aubrion, G., Fontaine, A., Kerveillant, P., &(2010). Effects of catch crops, no till and reduced nitrogen fertilization on nitrogen leaching and balance in three long-term experiments. *Agriculture, Ecosystems & Environment*, *135*(4), 268–278. https://doi.org/10.1016/j.agee.2009.10.005

Decina, S. M., Templer, P. H., & Hutyra, L. R. (2018). Atmospheric inputs of nitrogen, carbon, and phosphorus across an urban area: Unaccounted fluxes and canopy influences. *Earth's Future*, *6*(2), 134–148. https://doi.org/10.1002/2017EF000653

Dodds, W. K., & Oakes, R. M. (2008). Headwater influences on downstream water quality. *Environmental Management*, *41*(3), 367–377. https://doi.org/10.1007/s00267-007-9033-y

Duncan, J. M., Welty, C., Kemper, J. T., Groffman, P. M., & Band, L. E. (2017). Dynamics of nitrate concentration–discharge patterns in an urban watershed. *Water Resources Research*, *53*, 7349–7365. https://doi.org/10.1002/2017WR020500

Dupas, R., Abbott, B. W., Minaudo, C., & Fovet, O. (2019). Distribution of landscape units within catchments influences nutrient export dynamics. *Frontiers in Environmental Science*, *7*, 43. https://doi.org/10.3389/fenvs.2019.00043

Dupas, R., Jomaa, S., Musolff, A., Borchardt, D., & Rode, M. (2016). Disentangling the influence of hydroclimatic patterns and agricultural management on river nitrate dynamics from sub-hourly to decadal time scales. *The Science of the Total Environment*, *571*, 791–800. https://doi.org/10.1016/j.scitotenv.2016.07.053

Dupas, R., Musolff, A., Jawitz, J. W., Rao, P. S. C., Jäger, C. G., Fleckenstein, J. H., et al. (2017). Carbon and nutrient export regimes from headwater catchments to downstream reaches. *Biogeosciences*, *14*(18), 4391–4407. https://doi.org/10.5194/bg-14-4391-2017

Eder, A., Strauss, P., Krueger, T., & Quinton, J. N. (2010). Comparative calculation of suspended sediment loads with respect to hysteresis effects (in the Petzenkirchen catchment, Austria). *Journal of Hydrology*, *389*(1), 168–176. https://doi.org/10.1016/j.jhydrol.2010.05.043

European Environment Agency EEA (2012). *Corine Land Cover*. Copenhagen, Denmark: European Environment Agency. Retrieved from https://land.copernicus.eu/pan-european/corine-land-cover

European Environment Agency EEA (2013). *DEM over Europe from the GMES RDA project (EU-DEM, resolution 25m)*. Copenhagen, Denmark: European Environment Agency. Retrieved from https://www.eea.europa.eu/data-and-maps/data/eu-dem

Ehrhardt, S., Kumar, R., Fleckenstein, J. H., Attinger, S., & Musolff, A. (2019). Trajectories of nitrate input and output in three nested catchments along a land use gradient. *Hydrology and Earth System Sciences*, *23*(9), 3503–3524. https://doi.org/10.5194/hess-23-3503-2019

Godsey, S. E., Kirchner, J. W., & Clow, D. W. (2009). Concentration–discharge relationships reflect chemostatic characteristics of US catchments. *Hydrological Processes*, *23*(13), 1844–1864. https://doi.org/10.1002/hyp.7315

Goodridge, B. M., & Melack, J. M. (2012). Land use control of stream nitrate concentrations in mountainous coastal California watersheds. *Journal of Geophysical Research*, *117*, G02005. https://doi.org/10.1029/2011JG001833

Gross, N. (1996). Farming in former East Germany: Past policies and future prospects. *Landscape and Urban Planning*, *35*(1), 25–40. https://doi.org/10.1016/0169-2046(95)00215-4

Gustard, A. (1983). Regional variability of soil characteristics for flood and low flow estimation. *Agricultural Water Management*, *6*(2–3), 255–268.

Haitjema, H. M. (1995). On the residence time distribution in idealized groundwatersheds. *Journal of Hydrology*, *172*(1–4), 127–146.

Hannappel, S., Köpp, C., & Bach, T. (2018). Charakterisierung des Nitratabbauvermögens der Grundwasserleiter in Sachsen-Anhalt. *Grundwasser*, *23*(4), 311–321.

Häußermann, U., Bach, M., Klement, L., & Breuer, L. (2019). *Stickstoff-Flächenbilanzen für Deutschland mit Regionalgliederung Bundesländer und Kreise - Jahre 1995 bis 2017 Methodik, Ergebnisse und Minderungsmaßnahmen. Umweltbundesamt*. Retrieved from https://www.umweltbundesamt.de/sites/default/files/medien/1410/publikationen/2019-10-28_texte_131-2019_stickstoffflaechenbilanz.pdf

Hirsch, R. M., Archfield, S. A., & De Cicco, L. A. (2015). A bootstrap method for estimating uncertainty of water quality trends. *Environmental Modelling & Software*, *73*, 148–166. https://doi.org/10.1016/j.envsoft.2015.07.017

Hirsch, R. M., Moyer, D. L., & Archfield, S. A. (2010). Weighted regressions on time, discharge, and season (WRTDS), with an application to Chesapeake Bay river inputs 1. *JAWRA Journal of the American Water Resources Association*, *46*(5), 857–880. https://doi.org/10.1111/j.1752-1688.2010.00482.x

Hope, D., Naegeli, M. W., Chan, A. H., & Grimm, N. B. (2004). Nutrients on asphalt parking surfaces in an urban environment. *Water, Air, and Soil Pollution: Focus*, *4*(2–3), 371–390. https://doi.org/10.1023/B:WAFO.0000028366.61260.9b

Hrachowitz, M., Soulsby, C., Tetzlaff, D., Dawson, J. J. C., Dunn, S. M., & Malcolm, I. A. (2009). Using long-term data sets to understand transit times in contrasting headwater catchments. *Journal of Hydrology*, *367*(3), 237–248. https://doi.org/10.1016/j.jhydrol.2009.01.001

Huber, C. (2005). Long lasting nitrate leaching after bark beetle attack in the highlands of the Bavarian Forest National Park. *Journal of Environmental Quality*, *34*(5), 1772–1779. https://doi.org/10.2134/jeq2004.0210

Inamdar, S. P., O'leary, N., Mitchell, M. J., & Riley, J. T. (2006). The impact of storm events on solute exports from a glaciated forested watershed in western New York, USA. *Hydrological Processes: International Journal*, *20*(16), 3423–3439. https://doi.org/10.1002/hyp.6141

Jawitz, J. W., & Mitchell, J. (2011). Temporal inequality in catchment discharge and solute export. *Water Resources Research*, *47*, W00J14. https://doi.org/10.1029/2010WR010197

Jiang, S., Jomaa, S., & Rode, M. (2014). Modelling inorganic nitrogen leaching in nested mesoscale catchments in central Germany. *Ecohydrology*, *7*(5), 1345–1362. https://doi.org/10.1002/eco.1462

Kohl, D. H., Shearer, G. B., & Commoner, B. (1971). Fertilizer nitrogen: Contribution to nitrate in surface water in a corn belt watershed. *Science*, *174*(4016), 1331–1334. https://doi.org/10.1126/science.174.4016.1331

Köhne, C., & Wendland, F. (1992). *Modellgestützte Berechnung des mikrobiellen Nitratabbaus im Boden*, Jülich: KFA.

Krause, P., Bäse, F., Bende-Michl, U., Fink, M., Flügel, W., & Pfennig, B. (2006). Multiscale investigations in a mesoscale catchment? Hydrological modelling in the Gera catchment. *Advances in Geosciences*, *9*, 53–61.

Krueger, T., Quinton, J. N., Freer, J., Macleod, C. J. A., Bilotta, G. S., Brazier, R. E., et al. (2009). Uncertainties in data and models to describe event dynamics of agricultural sediment and phosphorus transfer. *Journal of Environmental Quality*, *38*(3), 1137–1148. https://doi.org/10.2134/jeq2008.0179

Kuhr, P., Kunkel, R., Tetzlaff, B., & Wendland, F. (2014). Räumlich differenzierte Quantifizierung der Nährstoffeinträge in Grundwasser und Oberflächengewässer in Sachsen-Anhalt unter Anwendung der Modellkombination GROWA-WEKU-MEPhos. *FZ Jülich, Endbericht*, *25*. https://lhw.sachsen-anhalt.de/fileadmin/Bibliothek/Politik_und_Verwaltung/Landesbetriebe/LHW/neu_PDF/5.0_GLD/Dokumente_GLD/GROWA-WEKU_2014/Endbericht_2014-04-25.pdf

Kunkel, R., & Wendland, F. (2006). Diffuse Nitrateinträge in die Grund- und Oberflächengewässer von Rhein und Ems. *FZ Jülich, Reihe Umwelt/Environment*, *62*.

Lindner, M., Maroschek, M., Netherer, S., Kremer, A., Barbati, A., Garcia-Gonzalo, J., et al. (2010). Climate change impacts, adaptive capacity, and vulnerability of European forest ecosystems. *Forest Ecology and Management*, *259*(4), 698–709. https://doi.org/10.1016/j.foreco.2009.09.023

Lutz, S. R., Trauth, N., Musolff, A., Van Breukelen, B. M., Knöller, K., & Fleckenstein, J. H. (2020). How important is denitrification in riparian zones? Combining end-member mixing and isotope modeling to quantify nitrate removal from riparian groundwater. *Water Resources Research*, *56*, e2019WR025528. https://doi.org/10.1029/2019WR025528

Majumdar, D., & Gupta, N. (2000). Nitrate pollution of groundwater and associated human health disorders. *Indian Journal of Environmental Health*, *42*(1), 28–39.

Mayer, P. M., Reynolds, S. K., McCutchen, M. D., & Canfield, T. J. (2005). Riparian Buffer width, vegetative cover, and nitrogen removal effectiveness: A review of current science and regulations (Vol. 27, Washington, DC:). US Environmental Protection Agency.

McLenaghen, R. D., Cameron, K. C., Lampkin, N. H., Daly, M. L., & Deo, B. (1996). Nitrate leaching from ploughed pasture and the effectiveness of winter catch crops in reducing leaching losses. *New Zealand Journal of Agricultural Research*, *39*(3), 413–420. https://doi.org/10.1080/00288233.1996.9513202

Meybeck, M. (1982). Carbon, nitrogen, and phosphorus transport by world rivers. *American Journal of Science*, *282*(4), 401–450.

Mikkelson, K. M., Bearup, L. A., Maxwell, R. M., Stednick, J. D., McCray, J. E., & Sharp, J. O. (2013). Bark beetle infestation impacts on nutrient cycling, water quality and interdependent hydrological effects. *Biogeochemistry*, *115*(1–3), 1–21. https://doi.org/10.1007/s10533-013-9875-8

Minaudo, C., Dupas, R., Gascuel-Odoux, C., Fovet, O., Mellander, P.-E., Jordan, P., et al. (2017). Nonlinear empirical modeling to estimate phosphorus exports using continuous records of turbidity and discharge. *Water Resources Research*, *53*, 7590–7606. https://doi.org/10.1002/2017WR020590

Montzka, C., Canty, M., Kunkel, R., Menz, G., Vereecken, H., & Wendland, F. (2008). Modelling the water balance of a mesoscale catchment basin using remotely sensed land cover data. *Journal of Hydrology*, *353*(3–4), 322–334. https://doi.org/10.1016/j.jhydrol.2008.02.018

Mueller, C., Krieg, R., Merz, R., & Knöller, K. (2016). Regional nitrogen dynamics in the TERENO Bode River catchment, Germany, as constrained by stable isotope patterns. *Isotopes in Environmental and Health Studies*, *52*(1–2), 61–74. https://doi.org/10.1080/10256016.2015.1019489

Musolff, A., Fleckenstein, J. H., Rao, P. S. C., & Jawitz, J. W. (2017). Emergent archetype patterns of coupled hydrologic and biogeochemical responses in catchments. *Geophysical Research Letters*, *44*, 4143–4151. https://doi.org/10.1002/2017GL072630

Musolff, A., Schmidt, C., Rode, M., Lischeid, G., Weise, S. M., & Fleckenstein, J. H. (2016). Groundwater head controls nitrate export from an agricultural lowland catchment. *Advances in Water Resources*, *96*, 95–107. https://doi.org/10.1016/j.advwatres.2016.07.003

Musolff, A., Schmidt, C., Selle, B., & Fleckenstein, J. H. (2015). Catchment controls on solute export. *Advances in Water Resources*, *86*, 133–146. https://doi.org/10.1016/j.advwatres.2015.09.026

Overbeck, M., & Schmidt, M. (2012). Modelling infestation risk of Norway spruce by *Ips typographus* (L.) in the lower Saxon Harz Mountains (Germany). *Forest Ecology and Management*, *266*, 115–125. https://doi.org/10.1016/j.foreco.2011.11.011

Padilla, F. M., Gallardo, M., & Manzano-Agugliaro, F. (2018). Global trends in nitrate leaching research in the 1960–2017 period. *The Science of the Total Environment*, *643*, 400–413. https://doi.org/10.1016/j.scitotenv.2018.06.215

Pellerin, B. A., Saraceno, J. F., Shanley, J. B., Sebestyen, S. D., Aiken, G. R., Wollheim, W. M., &(2012). Taking the pulse of snowmelt: In situ sensors reveal seasonal, event and diurnal patterns of nitrate and dissolved organic matter variability in an upland forest stream. *Biogeochemistry*, *108*(1–3), 183–198. https://doi.org/10.1007/s10533-011-9589-8

R Core Team. (2019). *R: A language and environment for statistical computing*. Vienna, Austria. Retrieved from https://www.R-project.org/

Rockström, J., Steffen, W., Noone, K., Persson, Å., Chapin, F. S., III, Lambin, E. F., et al. (2009). A safe operating space for humanity. *Nature*, *461*(7263), 472. https://doi.org/10.1038/461472a

Rode, M., Halbedel née Angelstein, S., Anis, M. R., Borchardt, D., & Weitere, M. (2016). Continuous in-stream assimilatory nitrate uptake from high-frequency sensor measurements. *Environmental Science & Technology*, *50*(11), 5685–5694. https://doi.org/10.1021/acs.est.6b00943

Rose, L. A., Karwan, D. L., & Godsey, S. E. (2018). Concentration–discharge relationships describe solute and sediment mobilization, reaction, and transport at event and longer timescales. *Hydrological Processes*, *32*(18), 2829–2844. https://doi.org/10.1002/hyp.13235

Sawyer, A. H., Kaplan, L. A., Lazareva, O., & Michael, H. A. (2014). Hydrologic dynamics and geochemical responses within a floodplain aquifer and hyporheic zone during Hurricane Sandy. *Water Resources Research*, *50*, 4877–4892. https://doi.org/10.1002/2013WR015101

Seitzinger, S., Harrison, J. A., Böhlke, J. K., Bouwman, A. F., Lowrance, R., Peterson, B., et al. (2006). Denitrification across landscapes and waterscapes: A synthesis. *Ecological Applications*, *16*(6), 2064–2090. https://doi.org/10.1890/1051-0761(2006)016[2064:DALAWA]2.0.CO;2

Seybold, E., Gold, A. J., Inamdar, S. P., Adair, C., Bowden, W. B., Vaughan, M. C., et al. (2019). Influence of land use and hydrologic variability on seasonal dissolved organic carbon and nitrate export: Insights from a multi-year regional analysis for the northeastern USA. *Biogeochemistry*, *146*(1), 31–49. https://doi.org/10.1007/s10533-019-00609-x

Silva, S. R., Ging, P. B., Lee, R. W., Ebbert, J. C., Tesoriero, A. J., & Inkpen, E. L. (2002). Forensic applications of nitrogen and oxygen isotopes in tracing nitrate sources in urban environments. *Environmental Forensics*, *3*(2), 125–130. https://doi.org/10.1006/enfo.2002.0086

Soulsby, C., Birkel, C., Geris, J., Dick, J., Tunaley, C., & Tetzlaff, D. (2015). Stream water age distributions controlled by storage dynamics and nonlinear hydrologic connectivity: Modeling with high-resolution isotope data. *Water Resources Research*, *51*, 7759–7776. https://doi.org/10.1002/2015WR017888

Strebel, O., Duynisveld, W. H. M., & Böttcher, J. (1989). Nitrate pollution of groundwater in western Europe. *Agriculture, Ecosystems & Environment*, *26*(3–4), 189–214. https://doi.org/10.1016/0167-8809(89)90013-3

Tarasova, L., Basso, S., Zink, M., & Merz, R. (2018). Exploring controls on Rainfall-runoff events: 1. Time series-based event separation and temporal dynamics of event runoff response in Germany. *Water Resources Research*, *54*, 7711–7732. https://doi.org/10.1029/2018WR022587

Thompson, S. E., Basu, N. B., Lascurain, J., Aubeneau, A., & Rao, P. S. C. (2011). Relative dominance of hydrologic versus biogeochemical factors on solute export across impact gradients. *Water Resources Research*, *47*, W00J05. https://doi.org/10.1029/2010WR009605

Trauth, N., Musolff, A., Knöller, K., Kaden, U. S., Keller, T., Werban, U., &(2018). River water infiltration enhances denitrification efficiency in riparian groundwater. *Water Research*, *130*, 185–199. https://doi.org/10.1016/j.watres.2017.11.058

Tuckey, J. W. (1977). Exploratory data analysis (Vol. 6, 131–160). Reading, MA: Addison-Wesley Publishing Company.

Van Meter, K. J., & Basu, N. B. (2015). Catchment legacies and time lags: A parsimonious watershed model to predict the effects of legacy storage on nitrogen export. *PLoS One*, *10*(5), e0125971. https://doi.org/10.1371/journal.pone.0125971

Van Meter, K. J., & Basu, N. B. (2017). Time lags in watershed-scale nutrient transport: An exploration of dominant controls. *Environmental Research Letters*, *12*(8) 084017. https://doi.org/10.1088/1748-9326/aa7bf4

Van Meter, K. J., Basu, N. B., & Van Cappellen, P. (2017). Two centuries of nitrogen dynamics: Legacy sources and sinks in the Mississippi and Susquehanna River Basins. *Global Biogeochemical Cycles*, *31*, 2–23. https://doi.org/10.1002/2016GB005498

Van Meter, K. J., Basu, N. B., Veenstra, J. J., & Burras, C. L. (2016). The nitrogen legacy: Emerging evidence of nitrogen accumulation in anthropogenic landscapes. *Environmental Research Letters*, *11*(3), 035014. https://doi.org/10.1088/1748-9326/11/3/035014

Whitehead, P. G., Wilby, R. L., Battarbee, R. W., Kernan, M., & Wade, A. J. (2009). A review of the potential impacts of climate change on surface water quality. *Hydrological Sciences Journal*, *54*(1), 101–123. https://doi.org/10.1623/hysj.54.1.101

World Meteorological Organization, WMO. (2008). *Manual on low-flow estimation and prediction*, (43–49). Geneva, Switzerland: World Meteorological Organization.

Wollschläger, U., Attinger, S., Borchardt, D., Brauns, M., Cuntz, M., Dietrich, P., et al. (2017). The Bode hydrological observatory: A platform for integrated, interdisciplinary hydro-ecological research within the TERENO Harz/central German lowland observatory. *Environmental Earth Sciences*, *76*(1), 29. https://doi.org/10.1007/s12665-016-6327-5

Yang, J., Heidbüchel, I., Musolff, A., Reinstorf, F., & Fleckenstein, J. H. (2018). Exploring the dynamics of transit times and subsurface mixing in a small agricultural catchment. *Water Resources Research*, *54*, 2317–2335. https://doi.org/10.1002/2017WR021896

Yang, X., Jomaa, S., Zink, M., Fleckenstein, J. H., Borchardt, D., & Rode, M. (2018). A new fully distributed model of nitrate transport and removal at catchment scale. *Water Resources Research*, *54*, 5856–5877. https://doi.org/10.1029/2017WR022380

Zhang, Q., Harman, C. J., & Ball, W. P. (2016). An improved method for interpretation of riverine concentration–discharge relationships indicates long-term shifts in reservoir sediment trapping. *Geophysical Research Letters*, *43*, 10215–10224. https://doi.org/10.1002/2016GL069945

Zink, M., Kumar, R., Cuntz, M., & Samaniego, L. (2017). A high-resolution dataset of water fluxes and states for Germany accounting for parametric uncertainty. *Hydrology and Earth System Sciences*, *21*, 1769–1790. https://doi.org/10.5194/hess-21-1769-2017